TAC-ENGINEERED T CELLS AS CARRIERS OF ONCOLYTIC VIRUS

INVESTIGATING THE USE OF T CELLS ENGINEERED WITH A T CELL ANTIGEN COUPLER (TAC) RECEPTOR AS CELLULAR CARRIERS OF ONCOLYTIC MARABA VIRUS

By LISA SARA NEWHOOK, B.M.Sc (HONS)

A Thesis
Submitted to the School of Graduate Studies in
Partial Fulfilment of the Requirement for the Degree

Master of Science

McMaster University

MASTER OF SCIENCE (2017) **McMaster University**
(Medical Sciences) **Hamilton, Ontario**

TITLE:	Investigating the use of T cells engineered with T cell antigen coupler (TAC) receptors as cellular carriers for oncolytic maraba virus
AUTHOR:	Lisa Sara Newhook, B.M.Sc (University of Western Ontario)
SUPERVISOR:	Jonathan L. Bramson, Ph.D
NUMBER OF PAGES:	xii, 94

Abstract

The field of immuno-oncology has made tremendous advances in the treatment of cancer. Adoptive cellular transfer (ACT) of tumor-specific T cells and oncolytic viruses (OVs) are powerful anti-tumor agents, but each modality faces significant challenges. Despite the promise of ACT against hematological malignancies, success has been limited in solid tumors. OVs preferentially lyse tumor cells, but have difficulty overcoming antiviral host factors when delivered systemically – therapeutic doses must therefore be quite high to achieve tumor delivery. One means of overcoming viral neutralization is by loading OV onto cellular carriers prior to treatment. Since engineered T cells and OVs both possess anticancer activity, and since viruses naturally associate with nearby circulating immune cells, employing T cells engineered with a T cell antigen coupler (TAC) receptor as viral carriers may offer an ideal combination. Our studies indicated that loading oncolytic maraba virus (MRB) onto T cells – engineered with a TAC receptor targeting HER2 – had no impact on the functionality or receptor expression of these T cells. OV loaded on the surface of these TAC-T cells enabled killing of a variety of tumor targets that may be otherwise resistant to TAC-T cell therapy. Efficacy remains to be elucidated *in vivo* using xenograft murine models due to the lack of a protective antiviral immune response, which ultimately resulted in encephalopathy. These observed toxicities were likely model-specific, as MRB has shown to be highly attenuated in healthy tissues of wild type models. While conceptually attractive, using TAC-T cells as viral carriers to deliver a multi-pronged, one-pot antitumor therapy directly to the site of the tumor requires further evaluation before considering human studies.

Acknowledgements

I must first begin by extending my most sincere gratitude to my supervisor, Dr. Jonathan Bramson. Thank you for giving me the opportunity to become a member of your lab and learn under your mentorship. The guidance and encouragement that you have provided me over the course of my graduate degree were invaluable to my success and the success of this project and thesis. Thank you for continuously believing in me and pushing me to reach my potential. To my committee members, Dr. Brian Lichty and Dr. Martin Stampfli, thank you for the insightful direction and expertise regarding my research and progress during my committee meetings.

To all the Bramson Lab members, both past and present, I am eternally grateful for your tremendous patience and support during my graduate studies. You provided a collaborative, professional, and engaging environment to work in. First, I would like to thank past Bramson Lab member, Dr. Heather VanSeggelen, for laying the groundwork from which this project stemmed and for training me in the fundamental techniques necessary to complete this research. I would like to extend a thank you to Joni Hammill, who taught me the mentality and skills required to become capable and confident working with mice. Ken Mwawasi, thank you for dedicating so much of your valuable time to teaching me *in vitro* techniques and listening to my endless contemplations regarding my project. Although not a Bramson Lab member, I also must thank Talveer Mandur for coming to my rescue when I was doubting my animal skills. In truth, every single person I

have encountered throughout my graduate studies at MIRC has been truly instrumental in my success.

To my family, I cannot even begin to express how grateful I am for all your encouragement throughout not only my thesis, but also the entirety of my schooling and life. I am so fortunate to be part of a family that supports me in any and all of my endeavours. Thank you for having faith in me – it was a constant source of self-belief to draw from. Thank you all for being proud of me, always. To my mother, especially, thank you for your patience and wisdom. I would not be the person I am today without your endless supply of love and motivation. You truly inspire me to reach for my potential.

Finally, to my friends, thank you for keeping me sane these past years. Your source of companionship is truly invaluable.

Table of Contents

List of Tables and Figures

List of Abbreviations and Symbols

α	alpha
β	beta
β-Me	β-mercaptoethanol
Δ	delta
γ	gamma
ε	epsilon
μ	micro
ACT	adoptive cellular transfer
APC	antigen presenting cell
CAR	chimeric antigen receptor
CD	cluster of differentiation
CNS	central nervous system
CRS	cytokine release syndrome
cRPMI	complete RPMI
CTL	cytotoxic T lymphocyte
CTLA-4	cytotoxic T lymphocyte antigen-4
DC	dendritic cell
DNA	deoxyribonucleic acid
DMEM	Dulbecco's modified Eagle medium
EDTA	ethylenediaminetetraacetic acid
effLuc	enhanced firefly luciferase
FACS	fluorescence-activated cell sorting
FBS	fetal bovine serum
FLuc	firefly luciferase
GFP	green fluorescence protein
HER2	human epidermal growth factor receptor 2
ICI	immune checkpoint inhibitors
IFN	interferon
i.p.	intraperitoneal
i.t.	intratumoral
i.v.	intravenous
IL	interleukin
IVIS	*in vivo* imaging system
LV	lentivirus
mAb	monoclonal antibody
MDSC	myeloid-derived suppressor cell
MEM	minimum essential medium
MFI	mean fluorescence intensity
MHC	major histocompatibility complex
MOI	multiplicity of infection
MRB	maraba

NGFR	nerve growth factor receptor
NK	natural killer
NOD	non-obese diabetic
NRG	NOD-*Rag1*^{null}*IL2rg*^{null}
OV	oncolytic virus
PBMC	peripheral blood mononuclear cell
PBS	phosphate-buffered saline
PD-1	programmed death-1
PD-LI	programmed death-ligand 1
PFA	paraformaldehyde
PFU	plaque-forming units
rh	recombinant human
RPMI	Roswell Park Memorial Institute
RT	room temperature
s.c.	subcutaneous
SD	standard deviation
T-VEC	talimogene laherparepvec
TAA	tumor-associated antigen
TAC	T cell antigen coupler
TCR	T cell receptor
TGF	transforming growth factor
TNF	tumor necrosis factor
TU	transducing units
VSV	vesicular stomatitis virus
WT	wild type

Declaration of Academic Achievement

The work depicted throughout this thesis is a culmination of the research efforts of myself over the past two years of my graduate studies at McMaster University. My supervisor, Dr. Jonathan Bramson, and I collaborated on the experimental design and data interpretation. All experimental details were planned and performed principally by myself with minor technical assistance provided by various lab members.

1.0 Introduction

1.1 Cancer

Cancer refers to a collection of related diseases, all characterized by the abnormal and unrestricted proliferation of cells in a localized area of the body. As the disease progresses, cancer cells can undergo metastases, whereby neoplastic cells migrate – via the circulatory and lymphatic systems – and invade distant tissues. While the field of medical oncology has made significant advances in the treatment and management of cancer, the disease remains one of the leading causes of death in developed countries. Indeed, within Canada alone, 30% of deaths are attributed to cancer and one out of every two people are expected to develop the disease in their lifetime[1], indicating a need for novel therapeutic strategies. Combinatorial strategies to cancer therapy have the potential to dramatically improve the outcome for cancer patients[2].

1.2 The Etiology of Cancer

Carcinogenesis is a process by which normal cells acquire progressive mutations, which allows them to proliferate uncontrollably and bypass homeostatic mechanisms that control cellular proliferation[3]. The processes that permit and regulate cellular growth and division during embryogenesis and healing are dysregulated during the cell's transformation into a neoplastic state. Notably, inheritable stochastic mutations occur in somatic cells, and a percentage of these accumulated changes result in the progression into a neoplastic state. Indeed, inheritable genetic mutations are a leading contributor in

oncogenesis, as is seen in cases of familial breast cancers[4]; however, exposure to chemical agents via lifestyle choices[5], tobacco use[6], or exposure to infectious agents, such as oncogenic viruses[7], also play a significant role in the development of various cancers. As cells acquire these mutations, become neoplastic, and induce tumorigenesis, they form a niche conducive to the growth of the tumor[8]. Many tumors may be a result of the transformation of merely one cell; however established tumors comprise a heterogeneous population of cells due to their inherent genetic instability[9]. Furthermore, cancerous cells recruit a stroma comprised of fibroblasts, myeloid cells, and vasculature, which contributes to tumor heterogeneity and growth[10]. Over time, malignant tumors will grow to a size at that impacts normal physiological processes. Since cancerous cells arise from the patient's own self, they are difficult to distinguish from normal, healthy tissues.

While primary tumors are largely treatable, many tumors will have undergone metastasis – a process by which malignant cells spread to distal sites of the body – by the time of clinical diagnosis[11]. Metastatic lesions are often more challenging to treat due to an increased genetic heterogeneity of the cancer[12]. Moreover, the presence of metastases is associated with poorer prognoses, as the cancer is more likely to impair a multitude of normal physiological functions[11]. Indeed, it is metastases, rather than primary tumors, that are responsible for most cancer deaths. As such, there exists a high demand for therapeutics capable of targeting systemically disseminated disease.

1.3 Conventional Cancer Treatments

The current standard of care is a limited selection between surgery, chemotherapy, radiation therapy[13], or, more recently, biologic therapy[14]. For localized and low-grade malignancies, surgery remains an effective means of treatment, as it allows complete resection of solid tumors, accurate grading of tumors, or – in cases where resection is not possible – debulking of the tumor[15]. However, many tumors develop in, or metastasize to, locations that are inaccessible by surgical means. Furthermore, various animal studies using both implanted and spontaneous tumors indicated that surgery contributes to the induction of metastases[16,17]. This phenomenon may be explained by the dissemination of tumor cells to distal sites during surgery[18], the release of growth factors (both systemically and locally)[19], and the suppression of immune system functions[20].

The advent of modern chemo- and radiotherapies allowed for the treatment of a more extensive range of cancers. Chemotherapy relies on the systemic delivery of cytotoxic or cytostatic chemicals that exploit the ability of cancerous cells to rapidly proliferate[21]. This broad class of therapeutics induces cellular death by different methods (either cell cycle-specific or non-specific), depending on whether the method of action relies on the cells being in a particular phase of the cell cycle. These chemical agents, however, target healthy, rapidly dividing cells in addition to their intended, malignant targets. Specifically, this therapeutic strategy affects white blood cells of the immune system, contributing to an immunocompromised state of the patient where they are susceptible to opportunistic bacterial and viral infections[22]. Radiotherapy delivers ionizing radiation to kill neoplastic

cells in a well-defined location[23]. This radiation subsequently induces DNA damage in the targeted cells, leading to their apoptosis. Radiation and chemotherapies are particularly useful in neo-adjuvant and adjuvant settings (pre- and post-surgical therapies, respectively), where they are used to target residual and/or metastatic disease[24]. However, since these modalities are also damaging to the DNA of healthy cells, patients who receive these compounds, while having some impact on the disease, are at risk for second, drug-induced cancers[25]. In fact, chemotherapies have shown to increase the risk of bone[26] and bladder[27] cancers, while radiation therapies are associated with an increased risk of sarcomas[26] and breast cancers[28].

There are a multitude of barriers to the success of current therapeutics. First, the inherent genetic instability of neoplastic cells results in intertumoral heterogeneity between patients whereby tumors of the same physiological origin and grading may respond differently to the same treatment[29]. Furthermore, the heterogeneity of cells within the tumor due to stochastic DNA errors in daughter cells results in subpopulations of tumor cells that are genetically distinct from one another. As such, there may exist a population of cells that is resistant to clinical intervention. Most treatment regimes today involve some form of combination therapy, as strategies that induce cell death by multiple approaches have the greatest chance of hitting all the tumor cells and prevent subsequent relapse of therapy-resistant tumors[30]. Even with successes observed with these conventional modes of therapy – or some combination of the three – patients with metastatic lesions generally do not experience lasting or durable responses. Therefore, both pre-clinical and clinical efforts

have been aimed at developing targeted therapeutics[i] capable of inducing cell death by different mechanisms.

1.4 The Immune System and its Role in Cancer

The concept of immunity was first documented in the 5th century BC by a Greek historian, Thucydides, in plague-stricken Athens. He had noted that individuals who had contracted the plague and survived were able to tend to the sick without risk of further infection[31]. This idea was later reintroduced with the concept of variolation[ii] and rudimentary vaccine strategies[iii] against the smallpox virus[32]. The immune system, however, does not solely exist to protect against invading pathogens; it also serves to protect an individual's own body from neoplastic disease – a concept now referred to as cancer immunosurveillance[33]. The hypothesis of immunosurveillance was introduced by Macfarlane Burnet who speculated that malignant cells develop regularly in humans and these malignant cells possess novel antigenic properties that induce an immune response[34]. This immune response, in turn, clears the malignant cells prior to any clinical evidence of existence. Indeed, hosts with impaired immune systems are at increased risk for developing

[i] Able to elicit tumor-specific killing in the absence of off-tumor toxicities[30].
[ii] The Chinese practiced variolation between the 14th and 17th centuries by exposing healthy people to scabs caused by the disease, generally through inhalation of powdered scabs. By the 1700s, the practice of variolation had spread to Turkey, where Lady Montagu had traveled after experiencing smallpox. She brought the practice into Western culture by inoculating her daughter against the disease[32].
[iii] Edward Jenner, in the 1760s, made an observation that dairy workers exposed to cowpox – a less pathogenic virus of the same family as smallpox – were resistant to smallpox infection. This observation led to the safer process of vaccination[32].

cancers - individuals with acquired immunodeficiency syndrome experience a greater incidence of Kaposi's sarcoma and other virally-induced cancers[35].

The hypothesis of cancer immunoediting, put forth by Schreiber *et al*., integrates the concept of immune escape with the aforementioned immunosurveillance hypothesis[33]. It maintains that the immune system not only protects the host from tumor progression, but also fosters the development of tumor growth by selecting for escape variants that can evade immunosurveillance. The cancer immunoediting hypothesis describes three stages: elimination, equilibrium, and escape. The first phase essentially refers to the immunosurveillance stage, whereby innate and adaptive immune cells cooperate to eliminate growing tumors before they are clinically evident[36]. If the mediators involved in this process are successful at eliminating these initial neoplastic cells, the host remains free of cancer. If, however, there are tumor variants able to avoid detection by immune cells, the tumor then enters equilibrium with the immune system, where continuous sculpting by the immune system results in immune selection of cells with reduced immunogenicity. During equilibrium, immunogenic tumor cells are destroyed as they replicate, while poorly immunogenic cells propagate, leading to the development of a tumor composed of cells that can evade the immune system, are resistant to mechanisms of immune-mediated killing, or are able to induce an immunosuppressive state within the tumor microenvironment. Neoplastic cells may become resistant to immune-mediated destruction by inducing anti-apoptotic mechanisms[37]. Furthermore, tumor cells can modulate the immunosuppressive nature of the tumor microenvironment by upregulating the expression

of inhibitory T cell ligands (such as PD-L1)[38], secreting suppressive cytokines (including transforming growth factor-β[39,40] and indoleamine 2,3-dioxygenase[41], and recruiting immunosuppressive immune populations (such as myeloid-derived suppressor cells (MDSCs)[42] and Regulatory T (T_{reg}) cells)[43]. At this point, the tumor has entered the escape phase and emerges as a progressive, clinically apparent tumor.

1.5 The Role of T Lymphocytes in Antitumor Immunity

T lymphocytes (from here on referred to as the T cell) are classified into two subtypes: $CD4^+$ and $CD8^+$ T cells – based on their coreceptor expression[44]. All T cells bear a receptor with unique specificity to an antigen, known as the T cell receptor (TCR). TCR binds to a defined peptide epitope presented in the context of a major histocompatibility complex (MHC) molecule. Two distinct classes of MHC exist – class I and class II – depending on the subset of T cells that it interacts with. Antigens presented in the context of MHC can be derived from cellular, bacterial, or viral protein sources.

T cells undergo development and maturation in the thymus, which gives rise to T cells with distinct specificities that are unable to respond to self[45]. The broad diversity of T cell recognition results from somatic recombination events where segments of the gene encoding the α and β chains of the TCR become rearranged, creating novel sequences[46]. This process gives rise to distinct T cell clones, ultimately creating a repertoire of cells capable of responding to a virtually any protein target. Consequently, T cells have the capacity to recognize self-derived antigens, which poses a risk of developing into

autoimmunity. A process known as central tolerance during thymic development prevents the generation of self-reactive T cell populations[47]. Through central tolerance, T cell precursors that have rearranged their TCR such that they can recognize self-antigen are eliminated.

Following recombination, T cells are assessed for the ability to bind antigen in the context of MHC[48]. These cells further undergo differentiation into $CD8^+$ or $CD4^+$ T cell subsets, depending on their ability to bind MHC class I or II, respectively[49]. Once these cells are fully matured, they egress from the thymus and enter secondary lymphoid organs, where they remain as naïve T cells until activation.

Naïve T cells[iv] are primed by antigen presenting cells (APCs) in these secondary lymphoid organs[50]. In particular, dendritic cells (DCs) sample antigens derived from tumor targets – either mutated or overexpressed proteins present in or on the tumor cell[51]. Upon antigen uptake, DCs will enter secondary lymphoid organs and prime naïve T cells[52]. Priming of T cells causes them to proliferate and differentiate into memory or effector cells. Memory T cells survive for extended periods in the circulation; they possess the ability to rapidly proliferate and respond to future antigenic stimulation. Effector T cells alternatively migrate to the tumor bed, where they elaborate their antitumor functions.

The most notable difference between $CD4^+$ T cells and $CD8^+$ T cells is in their functionality. $CD4^+$ T cells are involved in recruiting and coordinating the actions of other

[iv] T cell that has undergone maturation in the thymus, but has not yet encountered its cognate antigen[50].

immune cells, particularly $CD8^+$ T cells. These cells play a leading role in orchestrating the antitumor immune response[53]. This T cell subset secretes immunostimulatory chemokines, which recruit other innate immune cells, including natural killer (NK) cells and macrophages, to the site of the tumor. Furthermore, T_H1 T cells, a lineage of $CD4^+$ T cells, are involved in the activation and maturation of $CD8^+$ T cells[54]. However, not all $CD4^+$ T cells lineages are involved in facilitating the antitumor immune response. Rather, T_{regs} produce immunosuppressive cytokines, which serve to dampen the immune response[43]. Conversely, $CD4^+$ T cells have even shown the capacity to directly mediate anti-tumor efficacy[55].

$CD8^+$ T cells are essential for directly recognizing and abolishing both infected or, more notably, malignant targets – giving them the moniker, cytotoxic T cells (CTLs). Following recognition of these tumor-associated antigens (TAAs), CTLs induce necrotic and apoptotic pathways in tumor cells by a variety of mechanisms[56]. These cells release perforin and granzyme[v] via the granule-exocytosis pathway[57]. Cytotoxic cytokines, including IFNγ and tumor necrosis factor-α (TNFα), are also produced upon CTL activation. IFNγ induces the expression of MHC I on the surface of target cells, which serves to further sensitize tumor cells to T cell-mediated killing[58,59]. TNFα binds death receptors (TNF receptor 1 and 2) on tumor cells and enhances the activation of other T cells[60]. Additionally, TNFα increases vascular permeabilization to recruit other immune

[v] Perforin creates a hole in the target membrane, allowing granzyme entry into the target cell, where it initiates caspase-dependent apoptosis[57].

cells to the site of the tumor[61]. Finally, $CD8^+$ T cells induce apoptosis in their target cells by contact-dependent mechanisms – they express Fas ligand, a death receptor ligand, that binds to Fas on the surface of their target cells to induce caspase-dependent apoptosis[62].

1.6 Immuno-Oncology

Immuno-Oncology aims to harness the ability of immune cells to circulate, specifically recognize target cells, and elicit a durable and protective immune response. T cells possess qualities that render them ideal to utilize in a therapeutic, anti-cancer setting. In fact, it has been shown using tumor biopsies that the level and constitution of immune cell-infiltrates in the tumor correlates with the likelihood of therapeutic success in many cancers[63]. A multitude of strategies have been explored in which T cells are exploited to target tumor cells – either directly or indirectly. These strategies include biological therapies, adoptive transfer of tumor-specific T cells[64], and oncolytic viruses (OVs)[65]. These therapeutics have shown differing degrees of success at either clinical or experimental levels.

Biologics are therapeutic agents synthesized from living organisms and include cancer vaccines[66], monoclonal Abs (mAbs)[67], and cytokines[68]. This class of therapy is designed to restore, stimulate, or augment the immune response against neoplastic disease. One means of overcoming the sparsity of tumor-reactive T cells is to generate patient-derived anti-tumor responses through vaccination techniques employing viruses or DCs to encode or present, respectively, TAAs that prime endogenous tumor-reactive T cells[66]. To

date, cancer vaccines have only shown modest activity in the clinic, likely due to upregulated immunosuppressive mechanisms of the tumor cells in a direct and measured response to T cell attack[69]. Studies employing vaccines containing neoantigens have shown recent promise in clinical studies[70]. In fact, all six patients from one of these studies experienced durable responses for up to 32 months. T cells induced by vaccination, however, generally show slow response-kinetics, allowing the tumor time to adaptively respond to the pressures exerted on it by initial tumor-reactive T cells[71].

Immune checkpoint inhibiting mAbs function to antagonize receptors on the T cell surface that induce suppression[67,72]. These immune checkpoint inhibitors (ICIs) relieve inhibition of tumor-reactive – but functionally inert – T cells. Blockade of CTLA-4 or PD-1, both inhibitory receptors expressed by T cells, has shown to induce regression of otherwise treatment-unresponsive melanoma and increased survival in various other cancers[73,74,75]. Generally, the success of these therapies relies on the presence of anti-tumor T cells within the tumor microenvironment. Despite the success of ICI-mediated therapies, a small proportion of normal tissues express checkpoint receptor ligands, which contribute to mild – in some cases severe or lethal – off-tumor toxicities[76]. These toxicities are largely associated with the loss of autoimmune checkpoints in these healthy tissues, recruiting effector cells that cause healthy tissue damage. Furthermore, many tumors do not have immune cell infiltrate, providing no effector cells for the ICIs to act upon[63].

1.7 Adoptive Cellular Therapies: Engineering Antitumor Efficacy

A challenge to generating antitumor immunity is eliciting activity in an immunosuppressed environment. In addition to the immune suppression present within the tumor microenvironment, a limiting factor in the development of T cell immunity against tumors is immune tolerance, a collection of selection events that limit the development of T cells with receptors that recognize self. Autoimmunity results from the generation of T cells that are reactive against self, and there are mechanisms in place that eliminate these T cells from the host's immune cell repertoire. Specifically, central tolerance results in the elimination of T cells that react to self-derived antigens and peripheral tolerance results in the elimination of cells that are not only able to react to self-derived antigens, but also to neo-epitope-reactive T cells. Since tumor cells are self-derived, a consequence of this immune tolerance is a limited amount of natural T cells that recognize tumor antigens. Indeed, there is an extremely restricted repertoire of antigens available for recognition by T cells. These include neo-antigens (novel antigens produced because of genomic mutation)[77], germline-restricted antigens (antigens not expressed in healthy tissues, except during embryonic development)[78], or oncoviral antigens (antigens expressed by oncogenic viruses)[79].

Discoveries in the field of cancer immunotherapy have enabled manipulation of the immune system to overcome this limitation, such as the *de novo* generation of antitumor T cells. Here, tumor-specific T cells are administered to a patient in a process referred to as adoptive cell transfer (ACT). Indeed, it has been demonstrated that T cells elicit anti-tumor

responses when administered as ACT therapies[80]. It is likely that regressions observed in ACT protocols are due to the considerable number of tumor-specific T cells infused into the patient, which may overwhelm the adaptive response of the tumor[71].

ACT involves the *ex vivo* expansion of tumor-reactive T cells followed by infusion into a tumor-bearing host[64,81,82,83,84]. Once within the host, these cells migrate to the tumor site where they mediate their anti-tumor effector functions. Tumor-specificity of the T cells used in these ACT therapies can be achieved by several means, using either autologous T cells or T cells engineered for tumor recognition. Natural T cells, and T cells engineered with antigen-specific TCRs, require stimulation by cognate antigen in the context of MHC I. Tumor cells achieve immune escape by downregulating the expression of MHC molecules and tumor antigens[85], which limits the ability of autologous T cells used in ACT[86].

An alternate strategy for ACT involves engineering the patient's T cells with chimeric receptors able to induce T cell activation following direct interaction with tumor antigen in an MHC-independent fashion[87]. Chimeric antigen receptors (CARs) confer specificity for tumor targets and induce T cell activation upon antigen recognition by incorporating intracellular TCR signalling components fused to a tumor-specific binding domain. CAR-signaling occurs independently of the TCR complex engaging its cognate antigen, which bypasses the need for MHC:antigen presentation on tumor cells. There exist several different binding moieties for use as the antigen-binding domain in these receptors, which allows for the direct targeting of not only peptide molecules, but also carbohydrates

and glycolipids[88] expressed on the cell surface. CAR-engineered T (CAR-T) cells have shown considerable success in the treatment of melanoma[89] and hematological malignancies[90,91]. However, these engineered cells have also presented with considerable toxicities due to high affinity, artificial signaling receptors. Toxicities are either off-tumor/on-target, where they recognize target antigen expressed on normal tissue, or off-target, where they recognize healthy tissue in the absence of target antigen expression. Toxicities may even be attributed to CARs recognizing target within the tumor, as tumor burden at the time of infusion has been linked to severe cytokine release syndrome (CRS)[92]. Some clinical studies witnessed severe, and in some cases fatal, toxicities resulting from CRS (NCT02535364 & NCT02348216). In fact, a phase II clinical trial of Juno's JCAR015 (NCT02535364) was halted due to five patient deaths from CAR-related toxicities. The artificial nature of these receptors results in unregulated activation of these cells, imparting the potential for off-tumor toxicities associated with CRS.

1.8 Oncolytic Virotherapy

The concept of using viruses to treat cancer is based on reports that cancer patients who contracted a viral infection would, on occasion, experience brief periods of regression[93,94]. There are several replicating viruses currently being evaluated in the clinic as antitumor therapies[95]. OVs are those that specifically infect, replicate in, and abolish malignant cells while avoiding normal, healthy tissues[96]. Tumor specificity of these viruses is achieved naturally, as is with reovirus[97] and Newcastle disease virus[98], or through genetic engineering, as in the case of vesicular stomatitis virus (VSV)[99] and herpes simplex virus[100].

Modifications to OVs endow them with enhanced oncolysis by further attenuating their replication in normal cells or increasing their replication in tumor cells[99,101]. These viruses may be additionally manipulated to improve tumor tropism[102] or regulate the antiviral immune response.

Tumor selectivity is commonly engineered through one of two strategies. First, the interferon (IFN) sensitivity of the virus can be enhanced. Normal cells respond to viral infection by activating the IFN pathway, which mediates viral shutdown[103]. Tumor cells, however, are normally defective in this process, allowing IFN-sensitive viruses to selectively replicate in and lyse tumor cells[99]. The surrounding, healthy tissue controls viral replication and spread through IFN signaling. Second, virulence genes can be removed from the viral genome to attenuate its replication in healthy cells. Many of the 'hallmarks of cancer' – described by Hanahan and Weinberg[3] – reflect the changes that a normal cell undergoes following infection with a virus. These hallmarks include avoiding immune destruction, sustaining proliferation, resisting cell death, and evading growth suppressors. By modifying these viruses to lack the ability to induce these cellular changes, the virus must rely on phenotypic complementation from the tumor cell to successfully replicate, providing it with cancer-selectivity[104].

OVs induce multiple mechanisms of cancer cell death[105]. Not only do they directly induce cellular lysis, but they also promote the destruction of the tumor vasculature[106] and stimulate bystander antitumor immunity[107]. OVs instigate both innate and adaptive immune responses by a variety of mechanisms. These viruses bear pathogen-associated molecular

patterns that are recognized by host mediators of innate immunity[108]. OVs further act to promote the recruitment of T cells and NK cells by affecting the cytokine composition within the tumor microenvironment[109]. Finally, OVs initiate adaptive antitumor immunity[110]. TAAs are released into the tumor microenvironment following immunogenic cell death of the infected cell, which are then taken up by APCs and presented in secondary lymphoid organs to activate the adaptive immune response against these antigens[107]. It is the multiple, complementary mechanisms of action of OVs that distinguishes this class of therapeutics from others, such as tumor vaccines and immune adjuvants. As such, this therapeutic strategy represents another means of circumventing the limited expansion of tumor-specific T cells.

These viruses have many beneficial characteristics that distinguish them from conventional therapeutics[111]. Since OVs induce cell death by multiple mechanisms, many of which are independent of programmed cell death, there is a low probability of therapeutic resistance emerging[30]. OVs have unique pharmacokinetics – due to *in situ* viral amplification, the viral dose delivered to the tumor increases over time – in opposition to conventional therapies[104]. OVs can also be equipped with transgene-encoded proteins, which serve to deliver cytotoxic payloads or immunostimulatory molecules following tumor replication. Many candidate genes, including IFNγ[112]and interleukin-2 (IL-2)[113], have been investigated in several preclinical studies and has shown some promise. Alternatively, safety features can be built in to these viral vectors, such as drug or immune

sensitivity. Taken together, these characteristics endow OVs with desirable therapeutic and safety profiles.

Rhabdoviruses, like VSV and Maraba virus, have several properties that make them appealing for use as OVs[101]. First, their small size and ability to replicate to high titers in mammalian cells make them ideal from a manufacturing perspective. These viruses replicate exclusively in the cytoplasm of cells, eliminating the risk for genotoxicities. The genomes of rhabdoviruses can be readily manipulated to include transgenes (therapeutic or reporter) or to engineer improvements. As the majority of rhabdoviruses do not infect humans, antibodies against these viruses will often be non-existent at the time of initial dosing. However, the adaptive response does evolve against these viruses following OV-administration[114], inhibiting the systemic spread of subsequent doses.

Maraba virus was originally selected as a candidate OV for its high cytolytic activity in different tumor lines, its high viral productivity, and large burst size[101]. Maraba virus was further genetically manipulated in its M and G genes – maraba-MG1 (MRB-MG1) – to both attenuate its replication in healthy cells and enhance the cytolysis of tumor cells. Attenuation of virus replication in normal cells was mediated by both IFN-dependent and -independent mechanisms. In these studies, MRB-MG1 demonstrated robust antitumor activity in both xenograft and syngeneic murine models. MRB-MG1 has shown to be highly attenuated when administered to healthy, wild type (WT) tissues[101] and safe when administered systemically to humans, with some treatment-related toxicities presenting as

mild flu-like symptoms[115]. Furthermore, MRB-MG1 is currently being investigated in phase I/II clinical trials as an OV vaccine (NCT02285816 & NCT02879760).

1.9 Cellular Carriers for Tumor-Delivery

Viruses can be delivered directly to the tumor bed via intratumoral (i.t.) injection. Indeed, phase II[116] and III[117] clinical trials have shown antitumor efficacy following i.t. injection. However, in cases of metastatic lesions and tumors that are not directly accessible, viruses must be delivered systemically via intravenous (i.v.) injection. Naked virus injected into the circulation does not exist as free-floating for long[118,119] – most particles are rapidly neutralized by antibodies[120], complement proteins[121], and scavenger cells[122]. Neutralizing Abs are of particular importance when considering therapeutic administration, as patients can develop antiviral adaptive immunity, either from pre-exposure to the WT virus or from repetitive dosing of OV[123]. Moreover, OVs lack the ability to localize specifically to tumors or to extravasate from the circulation. Therapeutic doses must therefore be quite high to overcome these host barriers and achieve tumor delivery, increasing the risk of toxicity.

Despite host barriers to viral spread, viruses do gain access to the circulation[124]. As soon as 30 minutes following i.v. injection of VSV in mice, the virus was found to be associated with the cellular fraction of harvested blood, as opposed to the serum. These viruses adhere to[125] or infect[126] nearby immune cells in the circulation without neutralizing their infectivity. This sequestration of virus protects it from host factors, allowing it to

spread throughout the host. Preclinical studies have demonstrated that viruses can be loaded onto, or into, several cell types without interfering with the biology of either virus or carrier[114,127,128]. Indeed, this delivery approach offers the potential to package OV, protect it from neutralization, and deliver it to the tumor site where it can mediate anticancer efficacy. The ideal cellular carrier should be tumor-reactive, protect its cargo from host antiviral factors, and possess its own therapeutic activity[129].

There are certain debates to whether the carrier cell should be able to amplify the virus itself or not[124]. If a viral vector is associated with a cell in the circulation, it is also subject to the fate of that cell. As such, any candidate cellular carrier must be able to deliver the virus to the site of the tumor. If the virus can replicate in its carrier cell, the kinetics with which the virus replicates in the cell must be compatible with the trafficking of the cell – this would ensure that virus would only be released at the site of the tumor. However, if the carrier cell also possessed its own antitumor efficacy, using cells susceptible to viral infection may diminish the therapeutic effect by reducing the number of therapeutic cells capable of eradicating the tumor. As OVs are replication-competent, the delivery of even a small dose of virus to the tumor should be sufficient to induce a productive infection.

Different cell types have been shown to deliver OVs to tumors by their capacity to target either tumor-specific antigens, biological properties associated with the tumor, or the anatomical location of the tumor[124,130]. The ideal cell carrier would recognize a target associated only with the tumor cell and absent from any other tissue. This specificity should therefore result in the cellular carrier trafficking to the site of the tumor, where the OV is

released. T cells are ideal cellular candidates for this process, as they have the capacity to explicitly recognize TAAs. In fact, the process of OV-loading is compatible with current ACT protocols using therapeutic T cells. The use of a cellular carrier that also possesses antitumor efficacy is particularly attractive as they would not only release a viral payload, but also mediate their own cytolytic effector functions. As such, OV-loading of tumor-specific T cells represents a rational strategy to induce multimodal cancer cell killing. Endogenous T cells have proven to be an effective means of delivering different OVs to tumors in several pre-clinical models of OV-delivery[128,131,132,133,134,135,136]. Furthermore, this combination has resulted in increased efficacy relative to either therapeutic alone. The combination of two different treatment modalities in a one-pot approach to cancer therapy has the potential to yield synergistic therapeutic benefits. Even in cases where adoptively transferred cells are functionally ineffective *in vivo*[137], the addition of OVs affords the potential for the therapeutic infusion to elicit efficacy[138]. This is important when considering that ACT therapy is arduous and expensive – OV-loading mitigates the risk of spending valuable resources on a potentially ineffective therapeutic bolus of cells.

2.0 Central Questions and Hypothesis

The concept of viral loading has proven to be broadly applicable to many different immune cell types including DCs[131], cytokine-induced killer cells[127], as well as transgenic T cells[132]. As stated previously, the tumor microenvironment is highly immunosuppressive and endogenous T cells have shown poor efficacy in the clinic. This platform would therefore likely benefit from the use of engineered T cells, especially in the context of an established tumor. Indeed, previous work in our lab showed that murine and human T cells engineered with a CAR targeting human epidermal growth factor receptor 2 (HER2) could be loaded with OV without impacting CAR expression, viability, or functionality *in vitro*[139]. Furthermore, these studies indicated that OV-loaded CAR-T cells could deposit virus onto tumor targets and this process may potentially enhance the efficacy of both approaches. The ideal cell carrier has yet to be identified – even endogenous or engineered T cells, which are highly specific for TAAs, have been shown to accumulate in normal, antigen-negative tissues – such as the lungs, spleen, and liver – following ACT[140,141].

Our lab developed a novel chimeric receptor – referred to as the T cell Antigen Coupler (TAC)[142]. Unlike CARs, the prototypical TAC does not incorporate signaling domains. Rather, it binds CD3ε of the TCR complex, redirecting the cell's native TCR upon recognition of target antigen. Cells engineered with the TAC receptor (TAC-T cells) have shown increased tumor cytolysis with reduced levels of cytokine production and toxicity in several tumor models (unpublished data), thereby increasing the safety profile of these cells compared to their CAR equivalents. The enhanced tumor cytolysis coupled with

increased safety imparted by this TAC receptor observed in preclinical models makes these cells promising for use in future clinical ACT studies and may be ideally suited for use as a cellular carrier.

OVs are attractive for use in conjunction with ACT, as they attack the tumor via pathways distinct from T cells[46] – this concept is important when attempting to overcome therapeutic resistance. T cells engineered with the TAC receptor have not yet been assessed as cellular carriers for the systemic delivery of OV. The addition of virotherapy, specifically MRB-MG1, to ACT via loading of TAC-T cells may enable targeting T cell-resistant variants and instigate additional, virus-mediated anti-tumor responses. In particular, combination therapies that mediate anti-tumor functions through distinct mechanisms have the potential to mediate synergistic efficacy[143,144]. It is important to consider when designing combination therapies that the effects of one do not interfere with the effects of the other used on its own. For example, most OVs are sensitive to the IFN response, particularly type I IFNs. IFNγ, although not type I, is produced by TAC-T cells and could negatively impact on viral replication.

Ultimately, this approach offers the potential to package OV, protect it from neutralization, and deliver it specifically to the site of the tumor. Furthermore, the presence of virus has the potential to target those cells that are inherently resistant to T cell-mediated cytolysis and T cell-mediated cytolysis will be able to target cells resistant to OV-therapy. We hypothesize that TAC-T cells can function as carriers of OV, the combination of which will enhance the antitumor properties of TAC-T cells both *in vitro* and *in vivo* in xenograft

models of human cancer. The ultimate goal of our research is to understand the interplay of combination therapies, focusing on rational therapeutic strategies.

3.0 Materials and Methods

3.1 Generation of Human Engineered T Cells

3.1.1 Lentivirus

Non-replicative, self-inactivating lentivirus (LV) was used to transduce primary human peripheral blood mononuclear cells (PBMCs). LV was produced via a third-generation system[145,146]. This system produces non-virulent lentiviral vectors that are biologically safe as a result of modifications to the genome of the virus. LV was produced by plating $8x10^6$ low passage HEK293TM cells in 3 x 15 cm dishes (NUNC) in 20 mL of HEK293TM culture media (DMEM, 10% heat-inactivated fetal bovine serum (FBS), 10mM HEPES, 2mM L-glutamine, 100 U/mL penicillin, and 100 uGu/mL streptomycin) 24 hours prior to transfection. One hour before transfecting HEK293TM cells, media was replaced with 12 mL of HEK293TM transfection media (DMEM, 10% heat-inactivated FBS, 10 mM HEPES, 2mM L-Glutamine, 0.1 mg/mL normocin). To transfect, packaging plasmids pRSV-Rev (6.25 µg; encodes *rev* gene, which regulates gene expression), pMD2.G (9 µg; encodes VSV-G, which confers cellular tropism), pMDLg-pRRE (12.5 µg; encodes *gag* and *pol* genes) and the transfer plasmid pCCL encoding the construct of interest (32 µg) were combined in 4 mL Opti-MEM (Gibco; cat:51985091) and incubated with another 4 mL Opti-MEM containing 120 µL Lipofectamine 2000 (Life Technologies, cat:11668027). HEK293TM cells were then transfected with 8 mL of this plasmid mixture per plate. Twelve to sixteen hours following transfection, 12 mL of HEK293TM culture

media supplemented with sodium butyrate (to final concentration of 1 mM) was used to replace HEK293TM transfection media.

Media was collected after 48 hours of incubation to collect lentiviral particles generated. Cellular debris in the collected media was centrifuged at 3000 rpm for 10 min, and the supernatant was filtered through a 0.45 µm PES filter. LV was concentrated using an Optima L-90K ultracentrifuge (Beckman Coulter) using an SW 32 Ti rotor (Beckman Coulter) at 28 000 RPM. The resulting pellet was resuspended in phosphate-buffered saline (PBS) at 4 °C and stored at -80 °C.

Viral titer was determined after one freeze-thaw cycle by serially diluting virus in HEK293TM culture media and transfecting $3x10^4$ HEK293TM cells. Specifically, HEK293TM cells were plated in 500 µL HEK293TM culture media in a 24-well plate (Falcon) and transduced with 0.5 mL media only (mock-transduced) or 0.5 mL of the lentiviral dilution (ranging from $2x10^{-3}$ to $2x10^{-6}$) after 3 hours. Three days following transfection, HEK293TM cells were harvested by vigorous pipetting and washed in fluorescence-activated cell sorting (FACS) buffer (PBS, 0.5% bovine serum albumin (BSA)) containing EDTA (2.5 mM). To determine viral titer in transducing units per mL (TU/mL), cells were assessed for the expression of the transduction marker, truncated nerve growth factor receptor (ΔNGFR) by staining for flow cytometry with an αNGFR-VioBrightFITC antibody (Miltenyi Biotec, cat:130-110). Staining was performed at room temperature (RT) in 50 µL of FACS buffer with 2.5 mM EDTA for 30 min. Cells were fixed for 15 mins at RT in 2% paraformaldehyde (PFA), washed, and filtered prior to being

run on a BD LSRFortessa flow cytometer. Data were analysed using FlowJo software to generate histogram plots with gating set on the unstained, mock-transduced cells. % $NGFR^+$ was determined by subtracting the % $NGFR^+$ value of stained, mock-transduced from stained, transduced samples. Finally, the titer was calculated using the formula:

$$\text{titer (TU/mL)} = (\#\text{ Cells plated} * \text{dilution factor} * \%NGFR^+) / 100.$$

Whichever dilution factor that resulted in a population of around 10% $NGFR^+$ was used in this calculation.

3.1.2 Culture and Transduction of Human Primary T cells

Human PBMCs, isolated either from healthy donors or leukapharesis products, were thawed at 37 °C and resuspended dropwise in 7 mL of T cell media (RPMI, 10% heat-inactivated FBS, 2 mM L-Glutamine, 10 mM HEPES, 0.5 mM sodium pyruvate, 1X non-essential amino acids (Life Technologies; cat:11140-050), 55 µM β-mercaptoethanol (β-Me), 100 U/mL penicillin, and 100 µg/mL streptomycin). Cells were pelleted at 1500 rpm for 5 mins and the supernatant was discarded. Cells were gently resuspended in 1-10 mL T cell media and counted on the hemocytometer or using a Countess II FL automated cell counter (ThermoFischer Scientific) This culture was either concentrated or diluted to a concentration of $1x10^6$ cells/mL in T cell media supplemented with recombinant human IL-2 (100U/mL final; Peprotech, cat:200-02) and IL-7 (10ng/mL final; Peprotech, cat:200-02). 100 µL of the cellular suspension was aliquoted per well in a 96-well U-bottom plate (tissue culture-treated, Falcon).

To activate and induce the proliferation of T cells, PBMCs were mixed with Human T-Activator αCD3/αCD28 Dynabeads (Life Technologies, cat:11131D) at a 0.8:1 ratio of beads to cells. Beads were washed in 1 mL Dynabeads wash (PBS, 0.1% BSA, and 2 mM EDTA, pH7.4) and placed on the MPS-C magnet (Life Technologies, cat:A13346). Dynabeads wash was removed and the beads were resuspended in T cell media supplemented with IL-2 (100 U/mL) and IL-7 (10ng/mL). 100 µL of the resuspension was added to each well containing 100 µL of PMBCs. Cells were incubated overnight at 37 °C at 5% CO_2.

18-24 hours following activation, T cells were transduced with LV. 110 µL of media was carefully pipetted off the top of these cells and LV was added to each well at the requisite multiplicity of infection (MOI) in 10 µL volumes of PBS. Depending on which construct the LV encoded, different MOIs were used to transduce these T cells. An MOI of 2 was used to transduce T cells with NGFR-encoding LV. LV encoding HER2-TAC of interest[vi] was added at an MOI of 10. After another 24 hours, 100 µL of cytokine-supplemented T cell media was added to each well. Cells were ready to be scaled when the diameter of the cellular cluster reached approximately 2-2.5 mm. At this point, the pellet was transferred into 1 mL of cytokine-supplemented T cell media. Cells were again ready for scaling once these wells approached 90-95% confluency, at which point three wells (of

[vi] Two different HER2-TAC constructs were used in these studies: (1) HER2-TAC containing murine UCHT1 mUCHT1-HER2-TAC or (2) HER2-TAC containing human UCHT1 (hUCHT1-HER2-TAC). Both receptors are functionally equivalent; however, transduction of human primary T cells with hUCHT1-HER2-TAC was higher than that observed in T cells transduced with LV encoding mUCHT1-HER2-TAC (unpublished data).

the same construct) would be pooled into a T-75 (oriented upright) into a volume of 6.4 mL of fresh, cytokine-supplemented media (10 mL total). Cells were counted every 2-3 days and fed or scaled accordingly to achieve a cellular density of $1x10^6$ cells/mL. These cultures were normally loaded with MRB virus and assessed on day 14 of culture.

3.2 Oncolytic Virus

3.2.1 Maraba Virus

MRB-MG1 – with mutations in its M (L123W) and G (Q242R) proteins – were encoded with reporter transgenes to detect viral replication *in vitro* and *in vivo*. MRB-MG1 expressing green fluorescent protein (MRB-MG1-GFP) was kindly supplied by Dr. Brian Lichty (McMaster University, ON). Stocks of MRB-MG1-GFP were stored at -80 °C in formulation Buffer (10 mM HEPES, 0.15 M NaCl, 4% Sucrose, pH 7.4) MRB-MG1 expressing Firefly Luciferase (MRB-MG1-FLuc) was generously provided by Dr. David Stojdl (University of Ottawa, ON). Viral stocks of MRB-MG1-FLuc were stored at -80 °C in PBS.

3.2.2 Viral Loading of Engineered T cells

To load T cells with Maraba virus, vector control- or HER2-TAC-engineered human T cells were first counted by hemocytometer and the requisite number of cells were collected by centrifugation. The supernatant was removed, leaving 2-3 mL of volume in which the pelleted cells were resuspended. MRB-MG1-FLuc or -GFP was added to the

cells at an MOI of 3 and the tubes were gently flicked to distribute the virus amongst the cells. As a control, cells were mock-loaded using an equivalent amount of formulation buffer. The tubes were then incubated at 37 °C for 3 hours. Loaded cells were washed four times in 10 mL of ice-cold PBS. OV-loaded cells were then resuspended in T cell media (for functional assays), PBS (for ACT), or FACS buffer (for staining), depending on their downstream use. OV-loaded T cells used in cell cytotoxicity, phenotypic, or functional assays were assessed immediately following loading or were resuspended in T cell culture media supplemented with IL-2 (100 U/mL) and IL-7 (10ng/mL) for 24 hours prior to being evaluated.

3.2.3 Preparing OV-loaded Cells for Plaque Assay

The number of infectious particles remaining associated with HER2-TAC-T cells following viral loading was determined by plaque assay. Specifically, cells were loaded as described in section 3.2.2 and resuspended to $1.25x10^6$ cells/mL in PBS. Tubes were placed at -80 °C until thawed for titration. To thaw, cells were removed from -80 °C and placed in a 37 °C water bath. Cells were resuspended by vortexing vigorously and diluted serially in base DMEM media prior to being used in a plaque assay.

3.2.4 Plaque Assay

Viruses were thawed on ice and diluted in formulation buffer to the desired working concentration. Remaining virus was aliquoted and stored at -80 °C. Prior to use, the titer of refrozen virus was determined by plaque assay.

Plaque assay of MRB-MG1 was performed on VERO cells. Briefly, $6x10^5$ VERO cells were seeded per well in a 6-well plate (Falcon) in VERO culture media (DMEM, 10% FBS, 2mM L-glutamine, 100 U/mL penicillin, and 100 µg/mL streptomycin). The following day, serial dilutions of either viral stocks or OV-loaded T cells thawed from -80 °C were prepared in base DMEM media (no serum). Media was removed from VERO cells and 100 µL of the dilution was added to the well in duplicate. 100µL of base DMEM was added to all wells and plates were incubated at 37 °C for 1 hour, rocking every 10-15 minutes. Infection solution was removed from wells and 2 mL of overlay (DMEM, 2mM L-Glut, 1% methylcellulose) was added to each well. Plates were incubated until plaques were visible.

Plaques were fixed with 500 µL of 100% methanol for 2-3 mins and stained with 1 mL giemsa (Sigma-Aldrich, cat:48900) diluted 1:10 in water for 5 mins. Plaques were counted, and the wells containing between 20-200 plaques were used in the following equation to calculate viral titer in plaque-forming units per mL (PFU/mL):

PFU/mL = (# of plaques) / (dilution factor * volume plated)

3.2.5 Antiviral Activity Assay

$5x10^4$ tumor cells were plated per well of a 96-well plate in 100 µL of cRPMI (RPMI, 10% FBS, 2mM L-glutamine, 55 nM β-Me, 10 mM HEPES, 100 U/mL penicillin, and 100 µg/mL streptomycin). Plates were incubated for 24 hours prior to treatment with recombinant human (rh) IFNβ/γ (Cedarlane, cat:CLCYT234/CLCYT206). Prior to treating

cells, rhIFNα/β was serially diluted two-fold in cRPMI. Media was aspirated from the wells of the 96-well plate and 100 µL of the rhIFNα/β dilution, or media only, was plated in duplicate. Plates were incubated for an additional 24 hours. Following this incubation, $5x10^5$ PFU of MRB-MG1-GFP were added to each well. Plates were incubated overnight and GFP production was visualized using the Typhoon Trio Plus Variable Mode Imager (GE Healthcare/Amersham Biosciences). Images were analyzed using ImageQuant TL 8.1 software (GE Healthcare Life Sciences).

3.3 Flow Cytometric Analysis

3.3.1 Phenotypic Analysis

The lentiviral vectors employed throughout these studies encode ΔNGFR as a marker of transduction. Cells were counted by hemocytometer or using a Countess II FL and $5x10^5$ cells were used in staining protocols. Cells were washed in 2 mL FACS buffer. Antibody cocktails were prepared and added to samples in 50 µL of FACS buffer with 2.5mM EDTA.

To measure HER2-TAC receptor expression, cells were first incubated for 30 mins at RT with 250 ng of recombinant HER2-Fc Chimera protein (R&D Systems, cat:1129-ER) per sample. Antibodies used in this research were: αCD4-AlexaFluor700 (eBioscience, cat:56-0048-82), αCD8-PerCp-Cy5.5 (eBioscience, cat:45-0088-42), αNGFR-BV421 (BD Pharmingen, cat:558116), αhuIgG (Fcγ)-PE (Jackson ImmunoResearch, cat:109-115-098), and αTCRαβ-FITC (BD Pharmingen; cat# 555547). Cells were fixed with 2% PFA for 15

mins at RT following staining. 35µm nylon mesh was used to filter the cells prior to running on either a BD LSRFortessa or a BD LSR II flow cytometer. Data were analyzed on FlowJo Software (FlowJo, LLC).

3.3.2 Intracellular Cytokine Staining

12-16 hours prior to stimulation, $5x10^4$ tumor cells were plated per well of a 96-well flat bottom plate in cRPMI, T cells were stimulated for 4 hours at 37 °C. $5x10^5$ T cells were added to the well in a volume of 50 µL of T cell media. Finally, 50 µL of T cell media with 0.2 µL Golgi plug (BD Biosciences, cat:555029) were added to the wells. 50 µL of 0.02 M EDTA was used to stop the stimulation. After 15 mins incubating at RT, cells were spun at 1500 rpm for 5 mins and kept overnight at 4 °C in 200 µL of fresh cRPMI.

The following morning, cells were stained for intracellular cytokine expression. Cells were pelleted by centrifugation at 1500 rpm for 5 mins. Supernatants from all spins were removed using a vacuum manifold (V&P Scientific, cat:VP-180) – all following wash steps, unless otherwise noted, were centrifuged under these conditions. Cells were washed twice with 200 µL of FACS buffer with 2.5 mM EDTA before staining with 50 µL per well of the primary, surface antibody cocktail for 30 mins at RT. Antibodies used in this cocktail were: αCD4-AlexaFluor (eBiosciences, cat:56-0048-82) and αCD8-PerCP-Cy5.5 (eBioscience 45-0088-42). Cells were washed twice with up to a total volume of 200 µL in FACS buffer with 2.5 mM EDTA following primary staining. Cells were permeabilized by incubating with 100 µL per well of Cytofix/Cytoperm (BD Biosciences, cat:554722) at RT

for 20 minutes. Cells were washed twice more in 1X Perm/Wash solution (BD Biosciences, cat:554723; total volume of 200ul). Cells were stained for 30 mins at RT with 50 µL using an intracellular cytokine cocktail prepared in 1X Perm/Wash. Antibodies used in the secondary cocktail were: αIFN-γ-APC (BD Pharmingen, cat:554702), αIL-2-PE (BD Pharmingen, cat:554566), and αTNF-α-FITC (BD Pharmingen; cat#:554512) Cells were subject to a final two washes in 1X Perm/Wash prior to resuspension in 200 µL of FACS with 2.5 mM EDTA. Cells were filtered and run on a BD LSRFortessa or a BD LSR II flow cytometer. Data were analyzed by FlowJo Software.

3.3.3 Infection Analysis

$1x10^6$ A549 (expresses HER2) or LOX-IMVI (lacks HER2 expression) tumor cells were plated in 2 mL cRPMI per well of a 6-well plate and incubated overnight. Media was removed from wells and $1x10^6$ HER2-TAC-T cells loaded with MRB-MG1-GFP were plated in 1 mL T cell media supplemented with IL-2 (100 U/mL) and IL-7 (10ng/mL). Cells were scaled every 48 hours. T cells were harvested at 24, 48, and 72 hours following tumour co-culture and washed in 2 mL FACS buffer + EDTA (2.5mM). T cells were stained for CD3 expression with αCD3:AF700 (BD Pharmingen, cat:557943). Following staining, cells were run on a BD LSRFortessa and data were analyzed with FlowJo software.

3.4 Cell Cytotoxicity Assays

Human A549, MDA-MB-231, OVCAR-3iv, and LOX-IMVI cells were used for *in vitro* cytotoxicity assays.

3.4.1 AlamarBlue Killing Assay

$1.25x10^4$ Tumor cells were plated in triplicate in a flat-bottom 96-well plate in 100 µL cRPMI. Additional wells were plated for tumor-only and media-only control wells. 16-18 hours following tumor cell plating, OV-loaded T cells were counted, resuspended in T cell media to $1x10^6$ cells/mL and serially diluted two-fold. These cells were then co-cultured with tumor cells at a range of effector:target ratios (from 0.25:1 to 8:1) by adding 100 µL of each dilution to the plate wells in triplicate. Control wells were given 100 µL of T cell media and plates were incubated overnight at 37 °C.

AlamarBlue Viability reagent (Life Technologies, cat:DAL1100) was diluted 1:10 in cRPMI prior to use and kept at 37 °C until it was added to the plate wells. A vacuum manifold was used to aspirate media from wells. Plates were further washed three times with warm PBS. 100 µL of 10% AlamarBlue solution was added to each well and incubated for 3 hours at 37 °C.

Fluorescence was read using a Tecan Safire plate reader (Tecan). The $\lambda_{excitation}$ and $\lambda_{emission}$ measurements parameters were set at 530 nm and 595 nm, respectively. Background emission was accounted for by subtracting the average media only value from all other well values. $\%_{cytotoxicity}$ was determined using the following formula:

$\%_{cytotoxicity}$ = ((untreated tumor cells – treated tumor cells) / (untreated tumor cells))*100%

3.4.2 Reporter Gene-Based Killing Assays

$5x10^4$ tumor cells expressing either GFP or enhanced luciferase (effLuf) were plated in triplicate in a flat-bottom 96-well plate in 100 µL cRPMI. Additional wells were plated for tumor-only and media-only control wells. 16-18 hours following tumor cell plating, OV-loaded T cells were counted, resuspended in T cell media to $4x10^6$ cells/mL and serially diluted two-fold. These cells were then co-cultured with tumor cells at a range of effector:target ratios (from 0.25:1 to 8:1) by adding 100 µL of each dilution to the plate wells in triplicate. Control wells were given 100 µL of T cell media. Plates were incubated overnight at 37 °C.

Fluorescence of the reporter gene was detected using a Typhoon imager. Data were analyzed using ImageQuant Software. Background emission was accounted for by subtracting the average media only value from all other well values. $\%_{cytotoxicity}$ was determined using the following formula:

$\%_{cytotoxicity}$ = ((untreated tumor cells – treated tumor cells) / (untreated tumor cells))*100%

3.5 Mice

3.5.1 Murine Models

Female NOD-*Rag1*^{null}*IL2rg*^{null} (NRG) mice were purchased from the Jackson Laboratory or bred in the Central Animal Facility at McMaster University. Female C57BL/6 mice were

purchased from Charles River Breeding Laboratories. All animal studies have been approved by the McMaster University Animal Research Ethics Board.

3.5.2 Tumor Challenge, ACT, and in vivo Tumor Monitoring

Virus-loaded, engineered T cells were prepared for i.v. injection on days 14 (ACT I) and 16 (ACT II) of T cell culture. $1x10^7$ viable T cells were injected in 200 µL of sterile PBS. In NRG murine models that employed a human xenograft model of metastatic breast cancer, MDA-MB-231, mice were challenged via subcutaneous (s.c.) injection of $1x10^6$ cells in 50 µL sterile PBS 28 days prior to ACT I. In models that used a human xenograft model of ovarian carcinoma, OVCAR-3iv[vii], $1x10^6$ cells were inoculated s.c. in 50 µL of sterile PBS 42 days prior to ACT I. Tumor volumes were measured every other day by taking length, width, and height measurements using calipers. Mice were monitored for signs of toxicity by measuring weight. Mice displaying signs of toxicity were supported with hydrogel, food on the cage floor, and placed on a heating pad at a low setting.

3.5.3 Bioluminescent Imaging

MRB-MG1 loaded on the surface of HER2-TAC-T cells used in ACT were encoded with a luciferase transgene to track virus replication *in vivo*. Following ACT, mice were imaged using the IVIS 200 Spectrum Imager (Caliper Life Sciences). Briefly, NRG mice were anesthetized using isoflurane USP (Baxter, cat:1001936040). Intraperitoneal (i.p.)

[vii] "iv" refers to the fact that this cell line was derived from tumor cells that had been passaged *in vivo* to select for variants that had more rapid growth.

injection of 100 mg/kg D-Luciferin (Perkin Elmer, cat:122799) was performed. Animals were maintained under isoflurane for 14 minutes before taking images using the "open filter" setting for 5s on the IVIS 200 Spectrum Imager (Perkin Elmer). Quantification of luminescent signal was performed using LivingImage v4.2 Software for MacOSX (Perkin Elmer).

3.5.4 Generation of anti-Maraba Immune Sera

To generate neutralizing immune sera against MRB-MG1, female C57Bl/6 mice were injected i.v. with two doses of $1x10^8$-$5x10^8$ PFU of MRB-MG1-FLuc one week apart. These mice were terminally bled 21 days following the second viral inoculation. Blood was collected by retro-orbital bleed using heparinase-free capillary tubes (Fischerbrand, cat:22-362574). Blood was collected in 1.5 mL Eppendorf tubes and incubated at RT for 30 min to allow coagulation to occur. Samples were spun at 1000 g at 4 °C for 10 minutes in a microfuge. The resulting supernatant – the serum – was transferred into a fresh tube and centrifuged again at 1000 g for 5 minutes to separate any residual red blood components. Sera were stored at -80 °C and injected i.p. at the adequate dilution in 300 µL of sterile PBS.

To confirm presence of neutralizing anti-MRB-MG1 antibodies, serum titration was performed using a neutralizing assay. VERO cells were plated to confluency in a 96-well, flat-bottom plate in 100 µL VERO culture media 12-16 hours prior to addition of serum. Sera were inactivated by incubating at 56 °C for 30 mins. Following heat inactivation, two-

fold serial dilutions of serum were prepared in VERO culture media (ranging from 1:4-1:8192). 50 µL of the dilution was incubated with 50 µL of VERO culture media containing $1x10^4$ PFU MRG-MG1-GFP for 30 mins @ 37 °C. Following incubation, media was removed from VERO cells and replaced with the incubation mixture. Plates were kept at 37 °C overnight and imaged the following day for viral replication. Fluorescence of the viral reporter gene was detected using a Typhoon imager. Data were analyzed using ImageQuant Software.

3.6 Tumor Cell Lines & Cell Lines Engineered for Reporter Gene Expression

3.6.1 Wild Type Cell Lines

The following human tumor cell lines were maintained in cRPMI: A549 (lung carcinoma), MDA-MB-231 (metastatic breast cancer), OVCAR-3iv and SKOV-3 (ovarian carcinomas), and the melanoma tumor cell line, LOX-IMVI. HEK293TM cells used to generate and titer LV were cultured in HEK293TM culture media. Finally, VERO cells, used in neutralizing assays and to titer OV, were maintained in VERO culture media.

3.6.2 Generating GFP-Expressing Tumor Cell Lines

Generating Lentiviral Vectors To create stably-expressing cell lines, we used a non-replicative, self-inactivating lentiviral system[146]. The reporter gene, EGFP was cloned into a lentiviral *pCCL* vector, which also confers Puromycin resistance. This gene of interest was placed under the control of the EF-1α promoter, while Puromycin resistance allowed

for the selection of transduced cells. Lentivirus was produced by four-plasmid transfection of HEK 293Tm cells as described previously[147,148]. Viral titers were determined using serial dilutions on 293Tm cells and evaluated by flow cytometric detection of GFP.

Human Cell Line Transduction Lentiviral transduction of human cell lines, including MDA-MB-231, and LOX-IMVI, were performed by myself and various members of our lab. In particular, each line was independently transduced with EGFP reporter gene constructs at an MOI of 3. Cells were cultured in media supplemented with Puromycin at a concentration specifically titrated for each cell line to select for cells expressing the gene of interest.

Assay Optimization The optimal seeding density of cells for use in this protocol was determined by plating an increasing number of MDA-MB-231 or LOX-IMVI cells expressing the reporter gene of interest in triplicate. These cells were incubated overnight to allow adhesion to the plate and assayed for the fluorescent expression of GFP using a Typhoon imager. Images were quantified using ImageQuant analysis. It was determined that for MDA-MB-231- and LOX-IMVI-GFP cells, fluorescent signal was linear up to a density of $1x10^5$ (**Figure 1A)** and $5x10^4$ (**Figure 1B**) cells/well, respectively.

To determine if detecting a decrease in reporter gene expression by these cell lines produced a measure of cytotoxicity that was equivalent to the standard AlamarBlue assay used in our lab, we tested these cell lines in parallel with WT lines using the appropriate signal detection parameters for each cell line. Human T cells were transduced

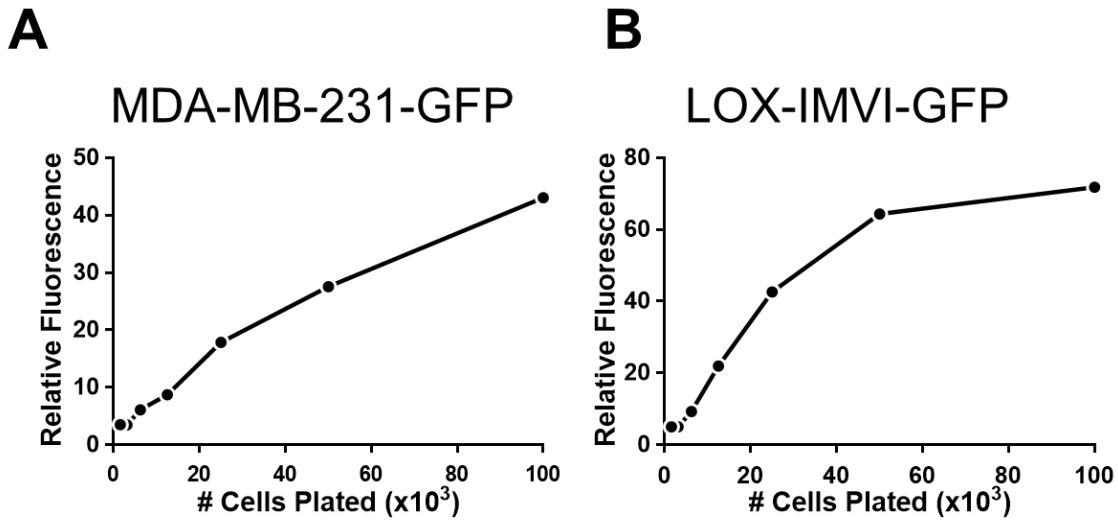

Figure 1: Reporter gene-expressing cell line titration. An increasing number of MDA-MB-231-GFP (A) or LOX-IMVI-GFP (B) tumor cells were plated in duplicate. After overnight incubation, cells were imaged for GFP expression using the Typhoon imager. Images were quantified using ImageQuant analysis. Data represent mean of one individual experiment.

with LV encoding a TAC specific for HER2 or vector control at an MOI of 10 or 2, respectively.

Vector control- or HER2-TAC-T cells were incubated in triplicate with HER2-expressing MDA-MB-231-WT or -GFP tumor targets at various effector to target ratios overnight. Plates containing MDA-MB-231-GFP cells were read on the Typhoon imager to detect fluorescence. WT cell lines were read on the Safire plate reader. Overall, we found the detection of a loss of GFP-reporter gene expression to be equivalent at determining cytotoxicity to the previous AlamarBlue assay (**Figure 2**, blue and green curves represent the Alamar Blue- and GFP-based assays, respectively).

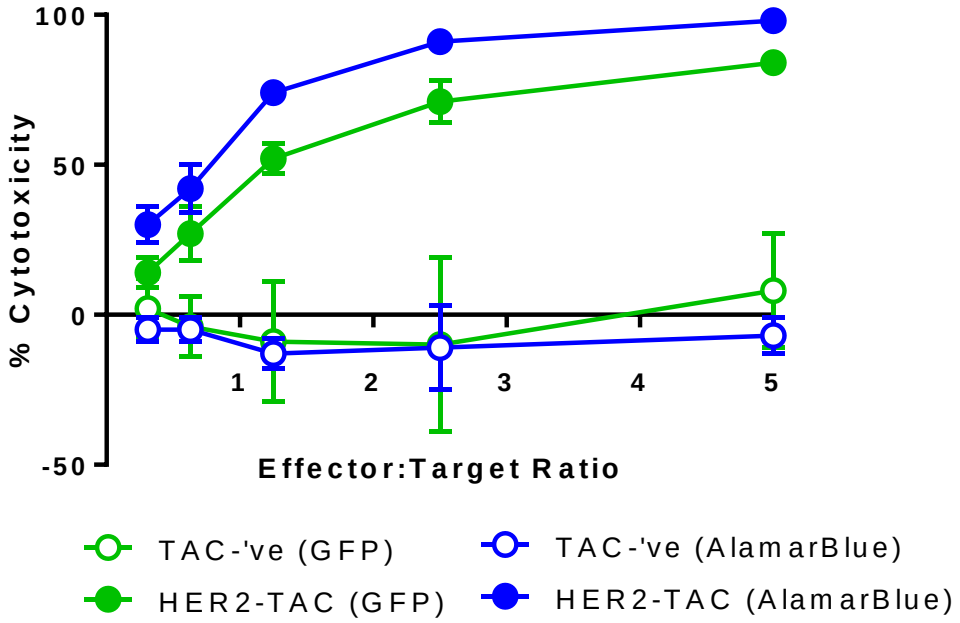

Figure 2: Head to head: cytotoxicity assay using AlamarBlue compared to GFP-reporter gene expression. Human T cells were engineered with HER2-TAC (closed circles) or vector control (open circles) and plated in triplicate with $5x10^4$ WT MDA-MB-231 (blue) or MDA-MB-231-GFP (green) cells at various effector:target ratios. After overnight incubation, cells were assessed for cytotoxicity by the designated method per cell line. Data represent mean ± SD of one independent experiment.

4.0 Results

4.1 TAC-T cells can be loaded with MRB-MG1

We first determined the amount of virus remaining associated with engineered T cells following loading with MRB-MG1. Human T cells were engineered with LV encoding a HER2-TAC receptor or vector control. Following expansion in culture, these cells were loaded with MRB-MG1-FLuc at an MOI of 3 or mock-loaded. Cells were washed and frozen at -80 °C prior to determining viral titer by plaque analysis on VERO cells. Loading with MRB-MG1 on the surface of engineered T cells resulted in few viral particles remaining associated with engineered T cells – only 36 or 56 PFU per $1x10^3$ vector control-T cells or TAC-T cells, respectively (**Table 1**). These values corresponded to an MOI of 0.036 following loading of vector control-engineered T cells or 0.056 following loading of TAC-T cells with MRB-MG1.

We next assessed whether OV-loaded TAC-T cells could transfer MRB-MG1 to tumor targets, resulting in tumor cytolysis. T cells engineered with TAC or vector control were loaded with MRB-MG1 as described and co-cultured at various effector:target ratios overnight with LOX-IMVI-GFP tumor cells. These tumor cells lack HER2 expression and, therefore, could only be killed by MRB-MG1-induced cytolysis. The effective MOIs of MRB-MG1 to LOX-IMVI tumor targets ranged from 0.018 to 0.288 for tumor cells incubated with OV-loaded vector control-T cells and between 0.028 to 0.448 for tumor cells incubated with OV-loaded TAC-T cells, according to the values determined in Table

Table 1: Viral titer of engineered T cells loaded with MRB-MG1. Engineered T cells were either mock-loaded or loaded at an MOI of 3 with MRB-MG1-GFP. Mock- or OV-loaded T cells were frozen post-wash to titer virus associated with these cells. Titer of MRB-MG1-GFP on $1x10^3$ engineered T cells was determined by plaque assay on VERO cells. Data represent mean of one independent experiment performed in duplicate.

Viral Titer (PFU)

	(Mock)	**+ MRB-MG1**
TAC –'ve	**0**	**36**
HER2-TAC	**0**	**56**

1. After 24 hours, cytotoxicity was determined by detecting and quantifying GFP expression in tumor cells. We observed no difference in killing when MRB-MG1 was delivered by vector control-engineered T cells compared to virus delivered by TAC-engineered T cells (**Figure 3**). These data supported that TAC-T cells can act as cellular carriers for delivery of MRB-MG1 and that the presence of the TAC does not affect transfer of MRB-MG1 to tumor cells.

4.2 The impact of OV-loading on TAC receptor expression and T cell functionality

We sought to determine if the presence of MRB-MG1 loaded on TAC-T cells impacted TAC receptor expression or function. We first determined if OV-loading altered surface HER2-TAC receptor expression *in vitro*. Engineered T cells were loaded at an MOI of 3 with MRB-MG1-FLuc or were mock-loaded. Following washing, cells were stained for changes in HER2-TAC receptor expression or incubated for another 24 hours prior to analysis. When cells were stained immediately following washing, there was no difference observed in the transduction of bulk T cells (**Figure 4A**). TAC-T cells, loaded at an MOI of 3, expressed HER2-TAC at levels equivalent to mock-loaded cells, as there was no difference observed in the expression of HER2-TAC in either $CD4^+NGFR^+$ or $CD8^+NGFR^+$ T cells (**Figure 4B**). When these cells were stained after overnight incubation following OV-loading, there was a small difference in the transduction of these cells, with a 13.8% loss in $NGFR^+HER2\text{-}TAC^+$ T cells (**Figure 4C**) when cells were loaded with MRB-MG1 (18.7%) compared to mock-loaded TAC-T cells (21.8%). Moreover, there was no loss of HER2-TAC expression in $CD4^+NGFR^+$ or $CD8^+NGFR^+$ T cells following

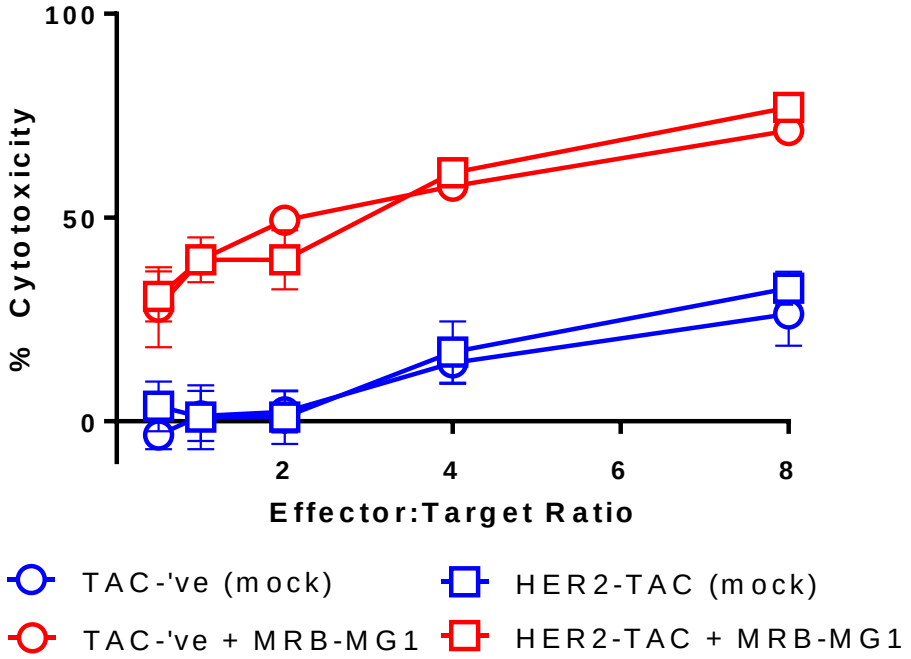

Figure 3: TAC-T cells transfer MRB-MG1 to tumor targets, resulting in tumor cytolysis. HER2-TAC- (squares) or vector control-engineered T cells (circles) were mock-loaded (blue) or loaded at an MOI of 3 with MRB-MG1-FLuc (red). OV-loaded T cells were co-cultured overnight at various effector:target ratios with LOX-IMVI-GFP tumor cells. Cytotoxicity was evaluated by detecting GFP expression as a surrogate of cellular viability. Fluorescence was visualized using a Typhoon imager and quantified with ImageQuant. Data represent one independent experiment performed in triplicate, presented as mean ± SD.

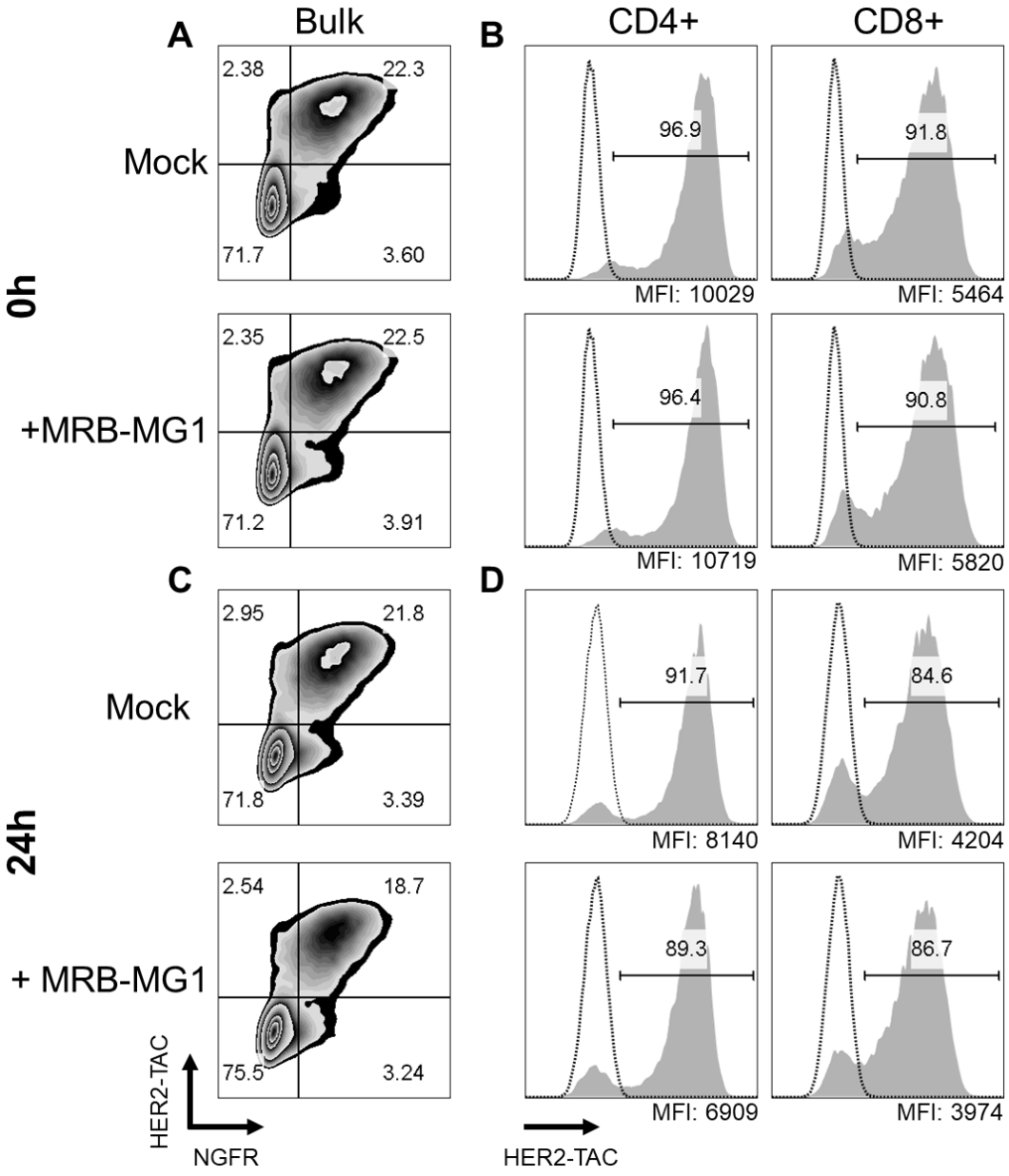

Figure 4: Phenotypic analysis of TAC-T cells loaded with MRB-MG1. Human T cells were transduced with HER2-TAC or vector control and loaded with MRB-MG1 at an MOI of 3 or mock-loaded. Following washing, cells were stained immediately (0h) for phenotypic analysis by flow cytometry (**A-B**) or returned to culture for 24 hours prior to analysis (**C-D**). Data were analyzed on FlowJo software. Zebra plots indicate transduction of bulk HER2-TAC-T cells (**A,C**). Histogram plots represent HER2-TAC expression in $CD4^+NGFR^+$ (**B,D**; left panels) or $CD8^+NGFR^+$ (**B,D**; right panels) HER2-TAC-T cells. MFI is indicated below each histogram. Results are representative of at least two independent experiments. MFI: mean fluorescence intensity

OV-loading (**Figure 4D**). These data suggest that OV-loading does not substantially impact upon surface HER2-TAC receptor expression.

We next investigated whether the functionality of TAC-T cells was affected by loading with MRB-MG1. TAC-T cells were loaded with MRB-MG1-FLuc at an MOI of 3 or were mock-loaded. The OV-loaded and mock-loaded TAC-T cells were either stimulated with HER2-expressing SKOV-3 tumor cells or LOX-IMVI tumor targets – which do not express HER2 – immediately after OV-loading. Additional groups of OV- and mock-loaded T cells were returned to culture for 24 hours prior to stimulation with either SKOV-3 or LOX-IMVI cells. Following 4 hours of SKOV-3 stimulation, cells were stained for cytokine production. When TAC-T cells were tested for cytokine production directly after loading, cytokine analysis revealed that loading of MRB-MG1 on TAC-T cells resulted in no change in cytokine production (**Figure 5A**). Mock- and OV-loaded $CD4^+$ or $CD8^+$ TAC-T cells produced both IFNγ, TNFα – or IL-2 (**Figure 6A**) – at equivalent frequencies following TAC-stimulation. When cells were incubated for an additional 24 hours, flow cytometric analysis revealed minimal changes in overall cytokine production (**Figure 5B)**. There was a small, but reproducible, difference observed in $TNF\alpha^+/IFN\gamma^+$ single producers and $TNF\alpha^+IFN\gamma^+$ double-producers in both $CD4^+$ and $CD8^+$ populations when TAC-T cells were loaded with MRB-MG1 compared to mock-loaded TAC-T cells. Loading of MRB-MG1 on TAC-T cells also resulted in no change in IL-2 production in $CD4^+$ or $CD8^+$ TAC-T cells loaded with MRB-MG1 compared to mock-

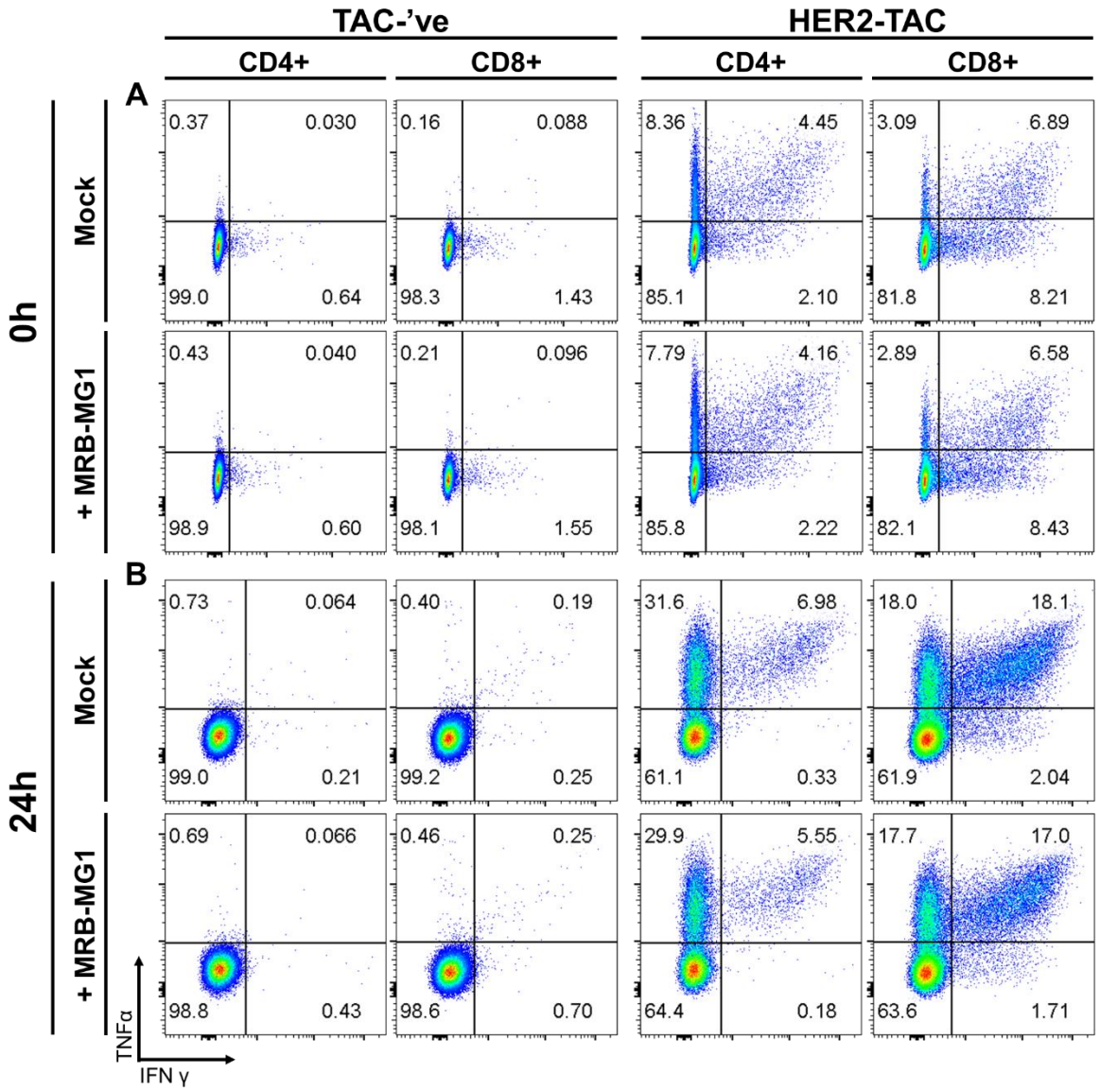

Figure 5: Evaluation of IFNγ and TNFα cytokine expression following loading with MRB-MG1. Human T cells engineered with vector control or HER2-TAC were loaded with MRB-MG1-FLuc at an MOI of 0 (mock) or 3, and washed. OV-loaded cells were assayed for cytokine expression immediately following washing (**A**) or were incubated for an additional 24 hours in culture prior to testing (**B**). Cells were stimulated with SKOV-3 tumor cells (express HER2) in the presence of brefeldin A prior to staining for IFNγ and TNFα. Cells were run on a flow cytometer and data were analyzed using FlowJo software, gated on $CD4^+NGFR^+$ or $CD8^+NGFR^+$ T cells. Data are representative of two independent experiments.

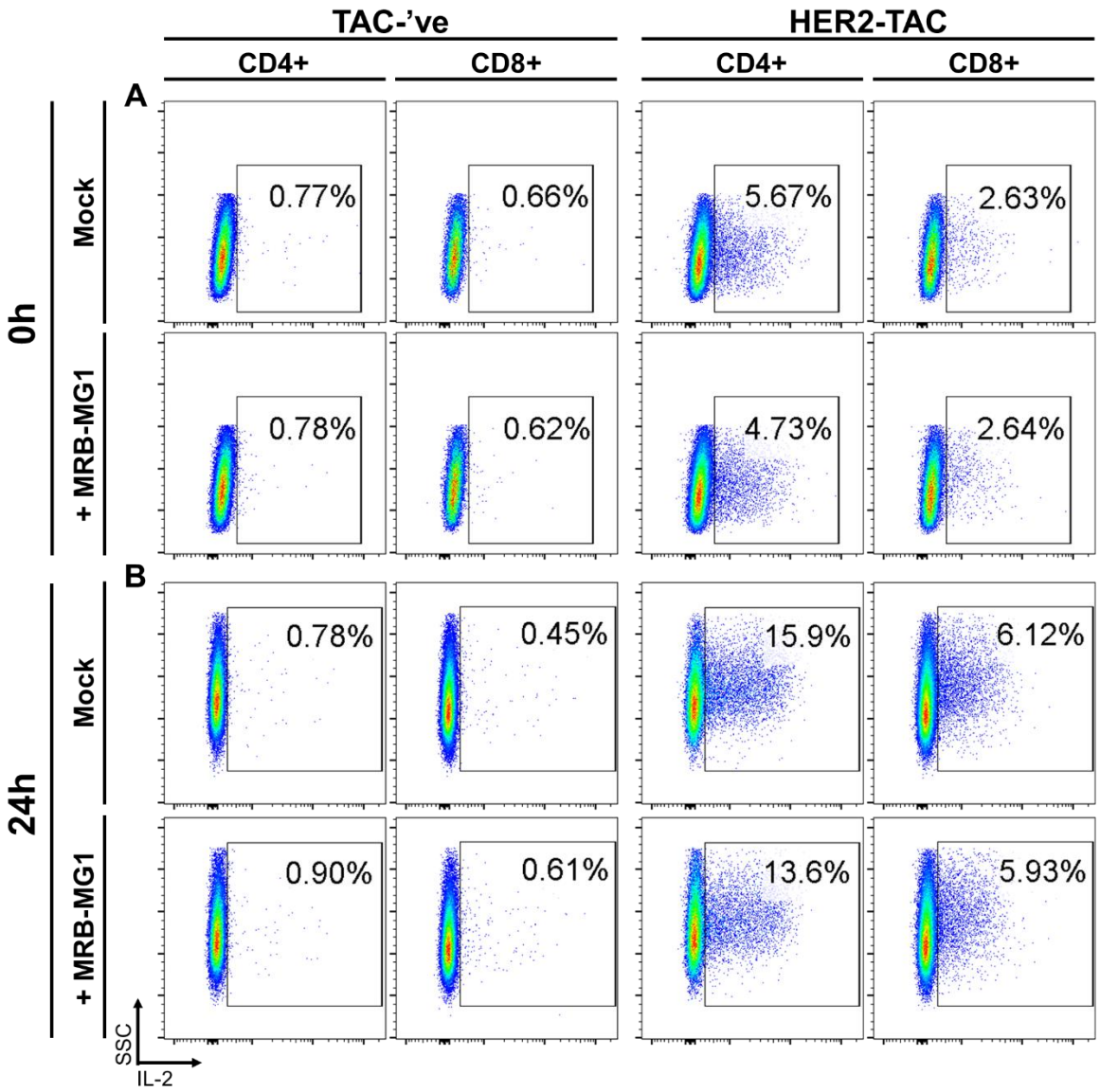

Figure 6: Evaluation of IL-2 cytokine expression following loading with MRB-MG1. Human T cells engineered with vector control or HER2-TAC were either mock-loaded or loaded with MRB-MG1-FLuc at an MOI of 3 and washed. Mock- and OV-loaded cells were assayed for cytokine expression immediately following washing (**A**) or were incubated for an additional 24 hours in culture prior to testing (**B**). Cells were stimulated with SKOV-3 tumor cells (express HER2) in the presence of brefeldin A prior to staining for IL-2. Cells were run on a flow cytometer and data were analyzed using FlowJo software, gated on $CD4^+$ or $CD8^+$ T cells. Data are representative of one independent experiment.

loaded TAC-T cells (**Figure 6B**). Overall, our data indicated that *in vitro* functionality of TAC-T cells was largely unchanged following loading with MRB-MG1.

We had previously demonstrated that loading of T cells with oncolytic rhabdovirus led to little productive infection as evidenced by lack of transgene expression[139]. Here, we repeated this analysis with MRB-MG1 and asked the additional question of whether stimulation through the TAC receptor would affect virus replication in our TAC T cells. Engineered T cells were loaded as described previously with MRB-MG1-GFP and co-cultured at a 1:1 effector:target ratio with A549 (HER2-expressing; **Figure 6**) or LOX-IMVI (lacks HER2 expression; **Figure 7**) tumor cells. These OV- and mock-loaded T cells were stained for CD3 expression and examined for GFP production by flow cytometry at 24, 48, and 72 hours following co-culture with tumor targets (**Figure 7**). We found infection of T cells to be highest at 24 hours following co-culture (**Figure 7A**). After 48 and 72 hours of co-culture, infection of T cells by MRB-MG1-GFP was found to be decreased (**Figure 7B,C**). In all cases, levels of infection were found to be lower than that observed in OV-loaded, vector control- or TAC-T cells co-cultured with A549 (**Figure 7**) or LOX-IMVI tumor cells (**Figure 8**), respectively. Taken together, our data indicated that loading TAC-T cells with MRB-MG1 had minimal impact on the engineered T cell product.

4.3 The impact of TAC-T cells on virus deposition

We further sought to determine whether TAC-T cells impacted upon MRB-MG1 deposition and replication following delivery by engineered T cells. As observed in the

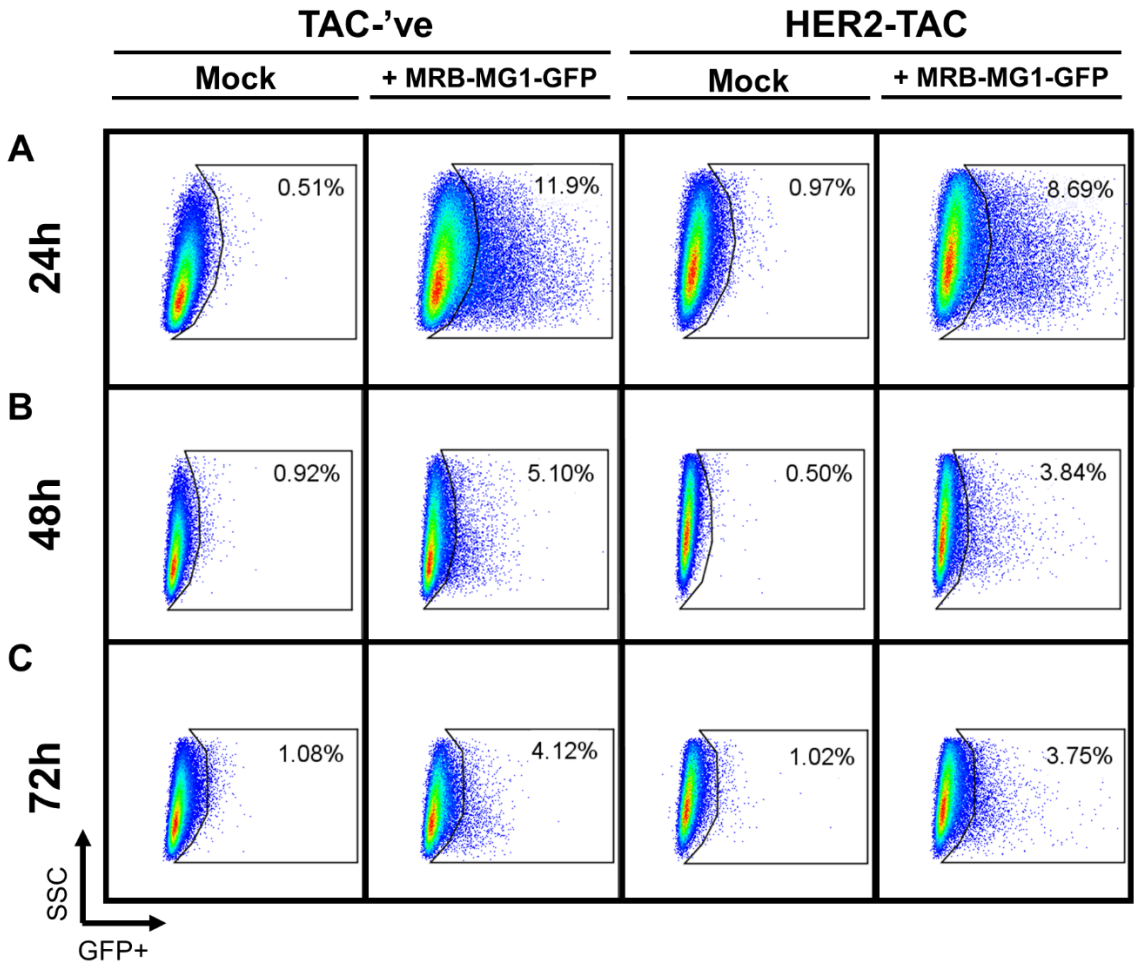

Figure 7: Analysis of MRB-MG1-GFP infection in OV-loaded TAC-T cells following antigen-stimulation. T cells engineered with HER2-TAC or vector control were loaded at an MOI of 0 (mock) or 3 with MRB-MG1-GFP. OV-loaded T cells were co-cultured at an effector:target ratio of 1:1 with A549 tumor targets for 24 (**A**), 48 (**B**), and 72 (**C**) hours, after which they were stained for CD3 expression and assessed for MRB-MG1-GFP infection by measuring GFP^+ cells using flow cytometry (gated on $CD3^+$ cells). Data represent one independent experiment.

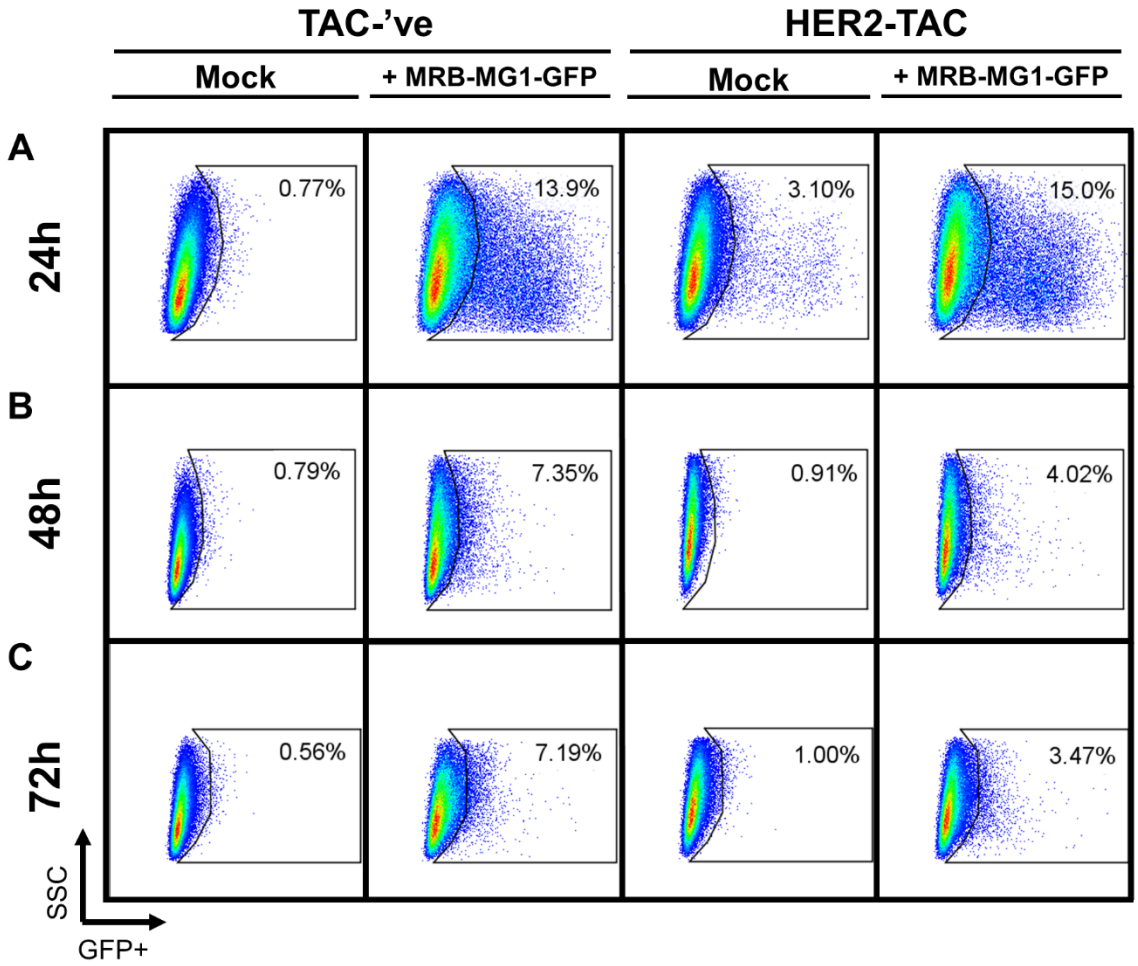

Figure 8: Analysis of MRB-MG1-GFP infection in OV-loaded TAC-T cells following co-culture with LOX-IMVI tumor cells. T cells engineered with HER2-TAC or vector control were loaded at an MOI of 0 (mock) or 3 with MRB-MG1-GFP. OV-loaded T cells were co-cultured at an effector:target ratio of 1:1 with LOX-IMVI tumor targets for 24 (**A**), 48 (**B**), and 72 (**C**) hours, after which they were stained for CD3 expression and assessed for MRB-MG1-GFP infection by measuring GFP^+ signal using flow cytometry (gated on $CD3^+$ cells). Data represent one experiment.

previous section, TAC-T cells produce cytokines – namely IFNγ – upon ligation with target antigen. IFNγ, while not a prototypical antiviral IFN, may impact upon viral replication. We therefore wanted to determine if activation through the TAC receptor would impair the ability of virus to be deposited onto tumor targets.

We first loaded engineered T cells with MRB-MG1-GFP and cultured these cells with various HER2-expressing tumor lines at an effector:target ratio of 1:1 for 24 hours – the effective MOI of MRB-MG1 to tumor targets cells was therefore 0.036 or 0.056 for targets incubated with OV-loaded vector control-T cells or TAC-T cells, respectively. Following co-culture, we evaluated virus transfer to the tumor lines by detecting GFP production (**Figure 9A**). Viral replication was found to be reduced in all tumor targets when deposited by TAC-T cells compared to virus deposited by vector control-T cells (**Figure 9B**).

While the reduction in GFP expression suggested impaired virus replication, one must also consider the possibility that TAC-mediated cytolysis reduced the numbers of cells available for virus replication. To directly assess whether IFNγ induces a protective response against MRB-MG1 in these cell lines, A549, MDA-MB-231, and OVCAR-3iv cells were treated with serial dilutions of recombinant human IFNγ or IFNβ (as a positive control) 24 hours prior to addition of MRB-MG1-GFP at an MOI of 10. Following overnight incubation, viral replication in tumor targets was evaluated by detecting GFP production. In all tumor cells, IFNγ was found to have equivalent antiviral activity to that provided by IFNβ (**Figure 10**). These data supported that IFNγ, produced by TAC-T cells

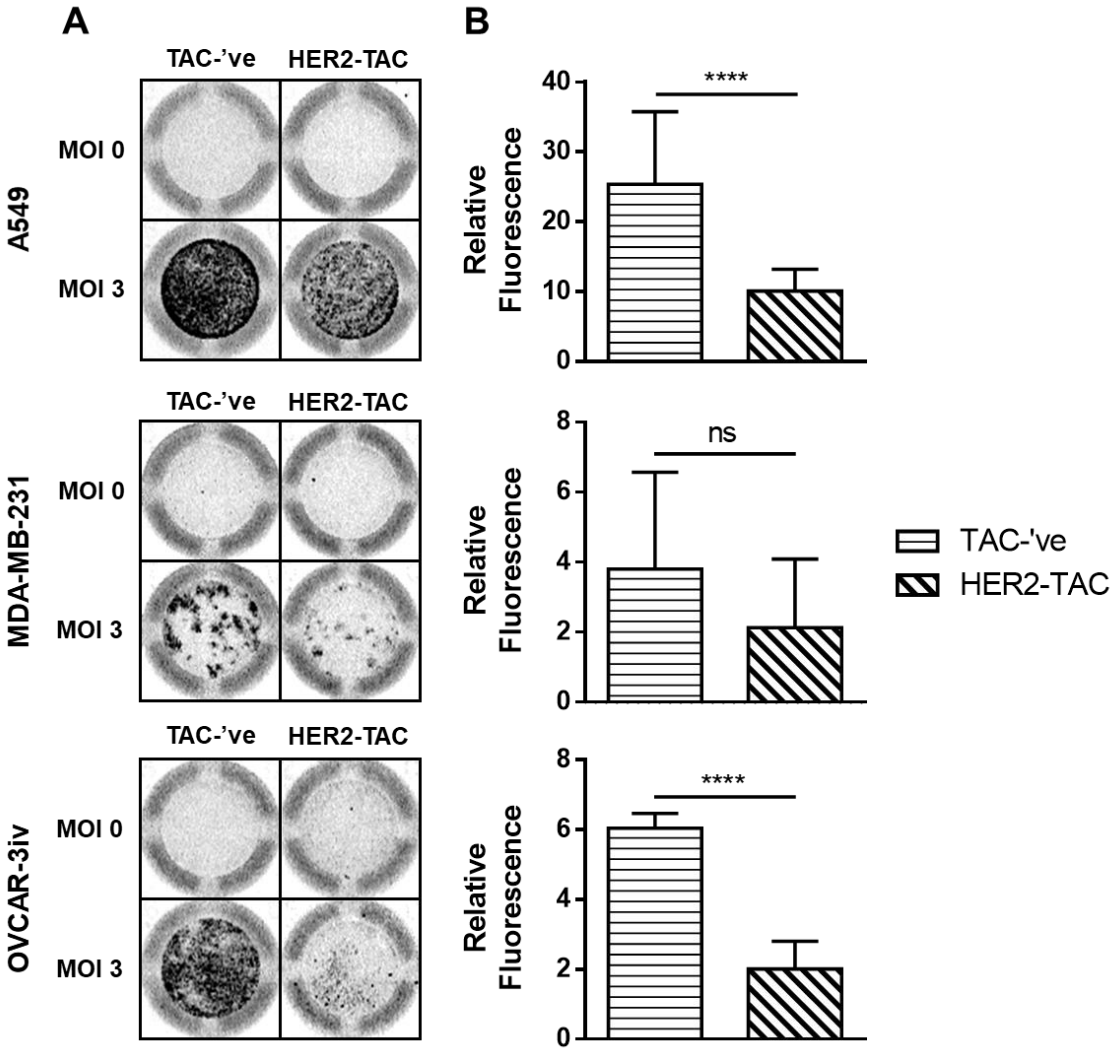

Figure 9: MRB-MG1 replication following deposition by engineered T cells. Human T cells engineered with TAC or vector control were loaded with MRB-MG1-GFP at an MOI of 3 or mock-loaded and co-cultured with (top) A549, (middle) MDA-MB-231, or (bottom) OVCAR-3iv cells overnight. Virus deposition was detected using the Typhoon imager to detect GFP expression (**A**). Images are representative of 2-3 independent experiments. GFP expression from cells incubated with TAC-T cells (horizontal lines) or vector control-T cells (diagonal lines) loaded at an MOI of 3 was quantified using ImageQuant software (**B**). Data are pooled from 3 independent experiments performed in triplicate and presented as mean ± SD, normalized to tumor-only wells. Unpaired t-test****:P<0.0001, ns:not significant.

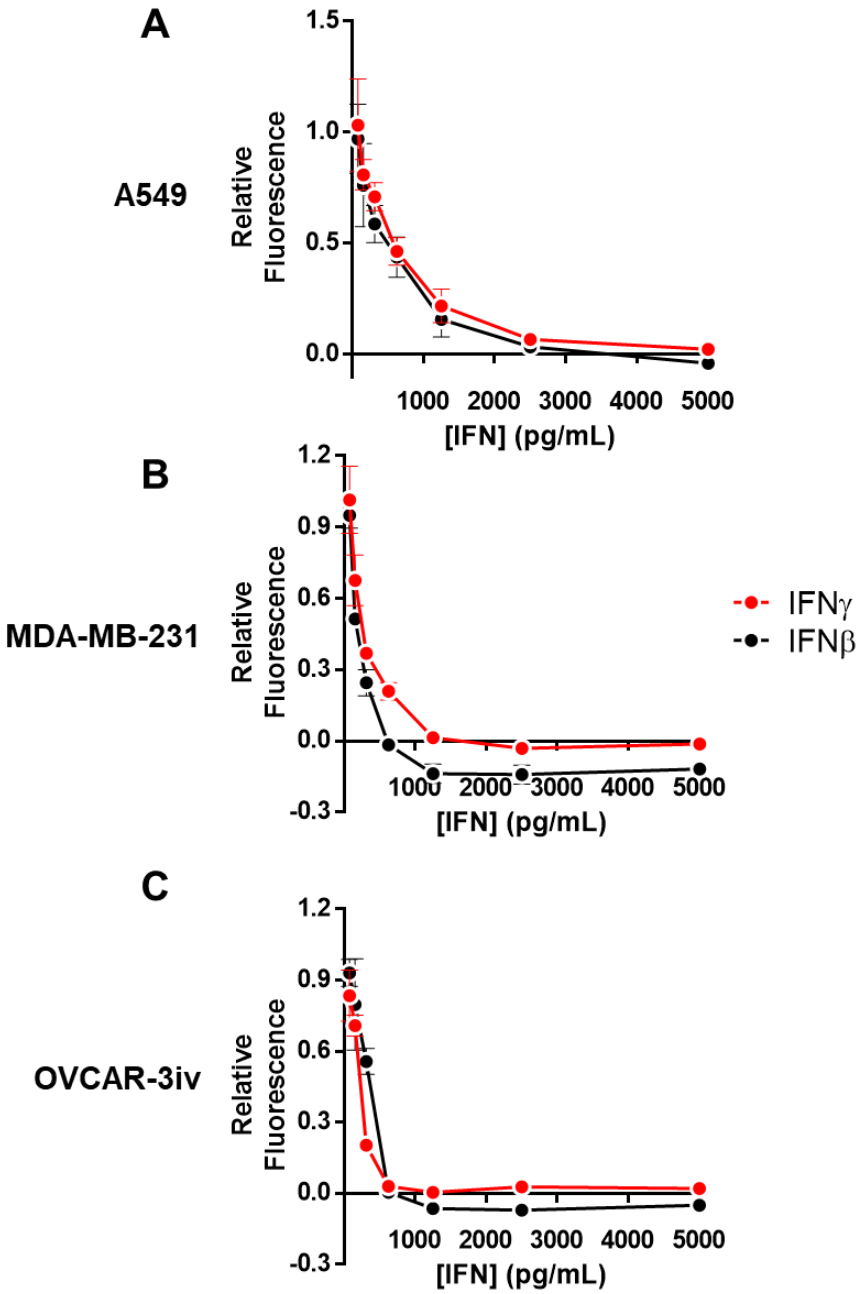

Figure 10. IFNγ impairs the ability of virus to replicate in vitro. A549 (**A**), MDA-MB-231 (**B**), or OVCAR-3iv (**C**) cells treated with serial dilutions of IFNγ (red) or IFNβ (black) were incubated with MRB-MG1-GFP overnight. GFP expression, as a marker of virus replication, was visualized using the Typhoon imager and quantified using ImageQuant. Data are representative of 2-3 independent experiments performed in triplicate and presented as mean ± SD, normalized to wells treated with no IFN.

after antigen-recognition, can impair replication of MRB-MG1 deposited by these engineered T cells.

To directly assess whether materials secreted by TAC-T cells could block virus replication following TAC-T cell stimulation, conditioned medium was prepared from co-cultures of TAC-T cells and HER2-expressing targets. A549 and OVCAR-3iv cells were incubated in the presence of different dilutions of medium or varying concentrations of IFNβ. Vector control-T cells loaded at an MOI of 3 with MRB-MG1-GFP were then added to targets at a 1:1 effector:target ratio, resulting in an effective MOI of 0.036. Viral replication was assessed in these targets using the Typhoon imager and quantified by ImageQuant. OVCAR-3iv tumor cells displayed the highest antiviral activity following treatment with TAC-conditioned media. A549 cells displayed antiviral activity following treatment with TAC-conditioned media (**Figure 11**, top panels), but to a lesser extent than was observed in OVCAR-3iv tumor cells (**Figure 11**, bottom panels). Taken together, these data indicated that the products of activation via the TAC receptor can inhibit viral replication *in vitro*.

We next characterized the impact of TAC-T cells on MRB-MG1-FLuc replication *in vivo*. Mice bearing s.c. MDA-MB-231 tumors were treated i.v. with two doses of TAC-T cells or vector control-engineered T cells – loaded with MRB-MG1-FLuc as described – 48 hours apart. The resultant dose of MRB-MG1 given to these mice was therefore approximately $3.6x10^5$ PFU and $5.6x10^5$ PFU per injection of $1x10^7$ vector control- or TAC-T cells, respectively, as calculated from the resultant titer determined in Table 1. Viral

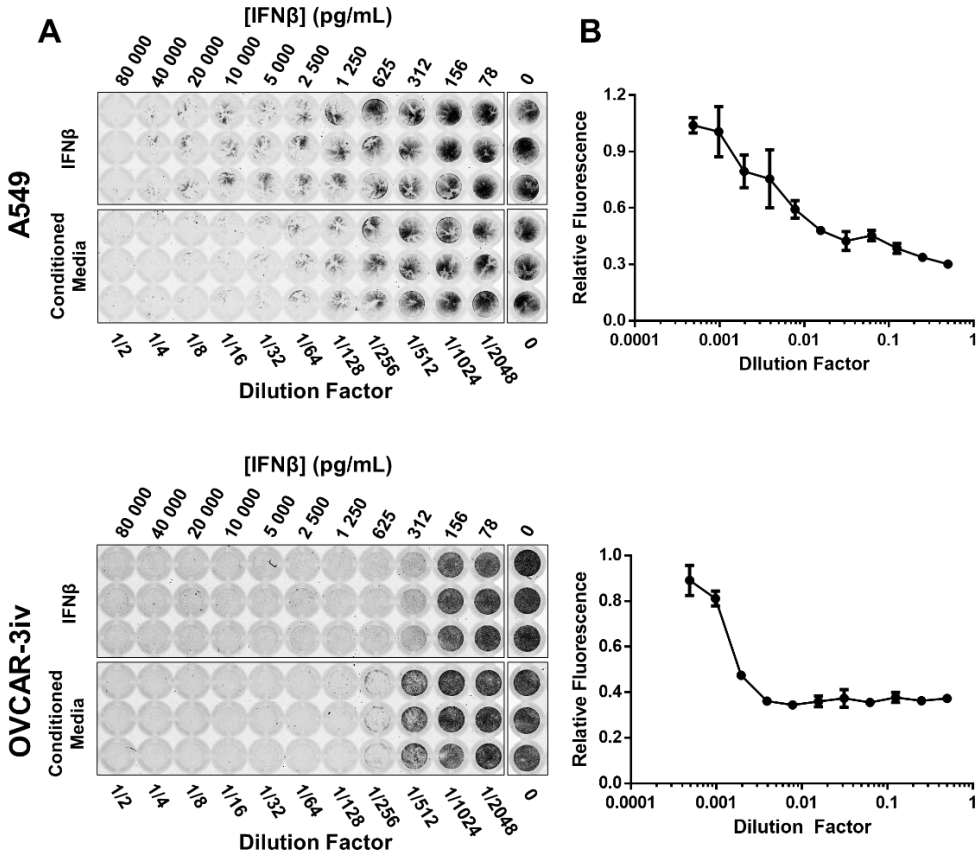

Figure 11. The by-products of TAC-T cell activation impair the ability of OV to replicate in vitro. HER2-TAC-T cells were co-cultured with tumor targets overnight and the supernatant (conditioned media) was collected. A549 (top panels) or OVCAR-3iv (bottom) tumor cells were treated with serial dilutions of conditioned media or known concentrations of IFNβ and incubated with MRB-MG1-GFP overnight. GFP expression, as a marker of virus replication, was visualized using the Typhoon imager (**A**). Fluorescence from wells treated with conditioned media were quantified with ImageQuant (**B**). Data represent 2-3 independent experiments performed in triplicate and are presented as mean ± SD, normalized to wells with no treatment.

replication was monitored following ACT by detecting FLuc production with IVIS imaging (**Figure 12A**). For both groups treated with OV-loaded T cells, viral replication peaked at 7 days post-ACT I (**Figure 12B**). However, mean luminescent signal from mice treated with TAC-T cells loaded with MRB-MG1-FLuc at this time point was determined to be $4.88x10^7 \pm 5.75x10^6$ p/s (**Figure 12B**, red squares), This signal was approximately two-fold lower than was observed in mice treated with OV-loaded, vector control-engineered T cells (**Figure 12B**; red circles, $9.16x10^7 \pm 1.61x10^6$ p/s**)**. Overall, our data demonstrated that OV-loaded TAC-T cells can transfer virus to tumor cells *in vitro* and *in vivo*. Our data further indicated that MRB-MG1 replication is negatively impaired by activation through the TAC receptor.

4.4 The impact of OV-loading on the therapeutic efficacy of TAC-T cells

Combination therapies using agents that employ different mechanisms of tumor cell destruction should enhance therapeutic efficacy. First, to evaluate the ability of OV-loaded TAC-T cells to enhance tumor cytolysis *in vitro*, we assessed cytotoxicity of OV-loaded engineered T cells in three different HER2-expressing tumor cell lines. These cell lines display varying degrees of susceptibility to TAC-mediated cytolysis, with A549 cells displaying the least sensitivity, MDA-MB-231 cells being intermediately sensitive, and OVCAR-3iv tumor cells having the greatest sensitivity (**Figure 13,** blue squares). These cells were also susceptible to MRB-MG1-GFP infection and cytolysis following deposition by OV-loaded, vector control-T cells (**Figure 13**, red circles). A549 cells supported the highest degree of viral replication compared to the other two cell lines (**Figure 9A**, top

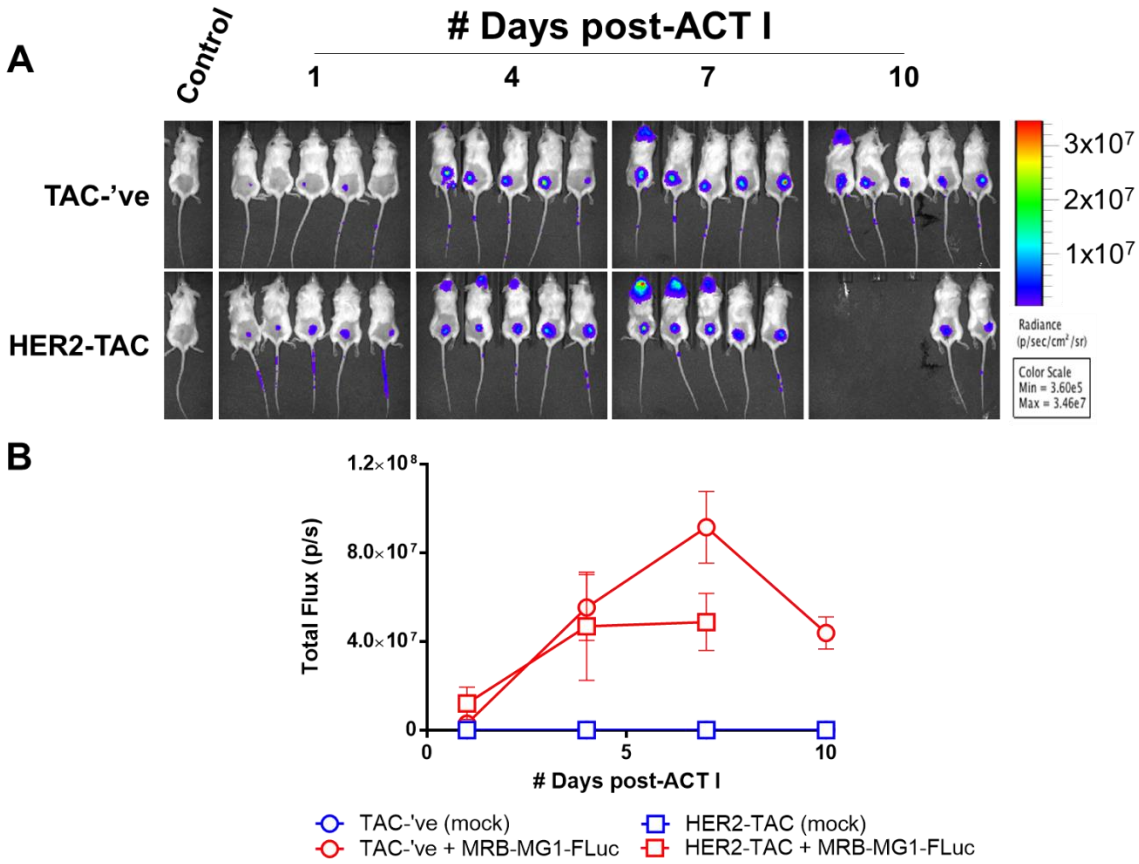

Figure 12: IVIS imaging of mice bearing MDA-MB-231 tumors treated with engineered T cells loaded with MRB-MG1-FLuc. Mice bearing s.c. MDA-MB-231 tumor cells were treated i.v. 48 hours apart with two doses of $1x10^7$ HER2-TAC- (squares) or vector control-T cells (circles), either loaded with MRB-MG1-FLuc at an MOI of 3 (red) or mock-loaded (blue). Following ACT, mice were monitored for viral replication by visualizing FLuc production via IVIS imaging (**A**). Total flux was calculated using LivingImage software (**B**). Data are presented as mean ± SEM (n = 5). All data represent three individual experiments.

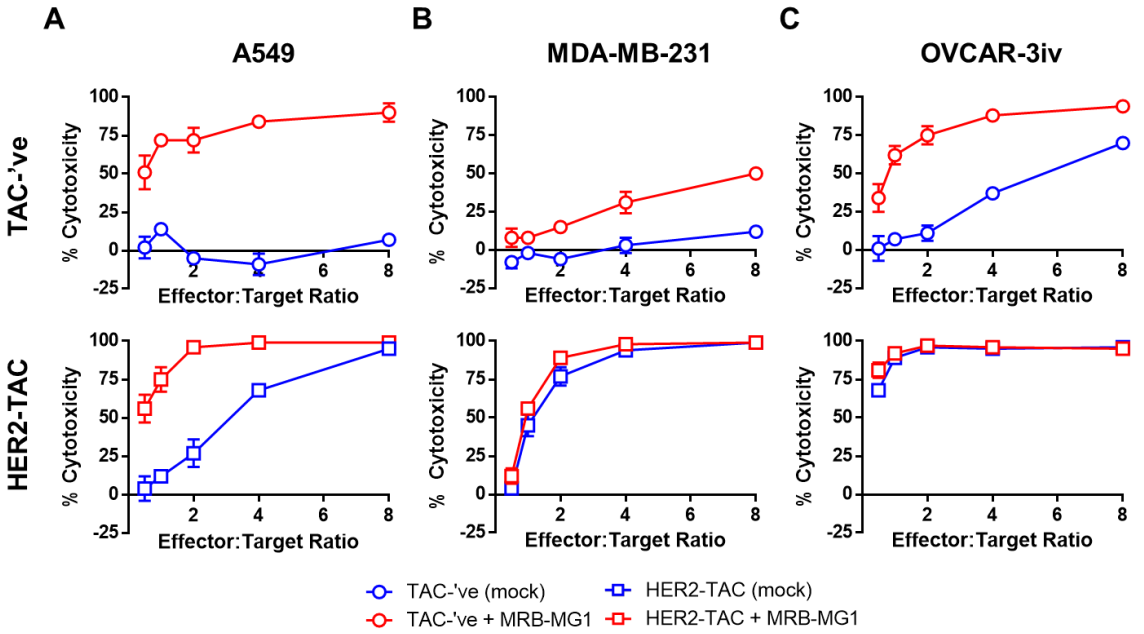

Figure 13: Cytotoxicity assay of engineered T cells loaded with MRB-MG1-GFP. HER2-TAC- (squares) or vector control-engineered T cells (circles) were loaded at an MOI of 3 with MRB-MG1 (red) or mock-loaded (blue). OV-loaded T cells were co-cultured overnight at various effector:target ratios with A549 (**A**), MDA-MB-231 (**B**), or OVCAR-3iv (**C**) tumor cells. Cytotoxicity was evaluated via AlamarBlue assay and plates were read using a Safire plate reader. Data are representative of 2-3 independent experiments performed in triplicate and presented as mean ± SD.

panels). MDA-MB-231 tumor cells were the most resistant to MRB-MG1-mediated cytolysis (**Figure 13B**). These differences in susceptibility to TAC- or OV-mediated cytolysis – as well as OV replication – provided a spectrum of tumor cell lines in which to assess the difference in therapeutic efficacy following loading of TAC-T cells with MRB-MG1.

We observed a reproducibly enhanced killing effect in A549 cells following co-culture with OV-loaded TAC-T cells (**Figure 13A**, red squares) relative to that of TAC-T cells alone (**Figure 13A**, blue squares). MDA-MB-231 cells are moderately sensitive to MRB-MG1 deposited by vector control-T cells (**Figure 13B**, red circles), but had no combinatorial effect when loaded onto TAC-T cells (**Figure 13B**, red squares). While OVCAR-3iv cells demonstrated sensitivity to MRB-MG1 deposited by vector control-engineered T cells (**Figure 13C**, red circles), robust killing by the TAC-T cells obscured any combinatorial effect (**Figure 13C,** red squares). These data suggest that the presence of virus did not impair the TAC-T cell's ability to selectively kill HER2-expressing tumor targets, nor did TAC-T cells impair the ability of MRB-MG1 to achieve tumor cell killing. Taken together, our data indicated that the addition of virus enables efficient killing of tumor targets that are otherwise resistant to TAC-T cell therapy.

We further investigated the efficacy of OV-loading in combination with ACT *in vivo* using MDA-MB-231 and OVCAR-3iv xenograft tumor models. NRG mice bearing s.c. tumors were treated i.v. with two doses of $1x10^7$ engineered T cells – loaded as described previously – 48 hours apart. Tumor volumes and weight were monitored

following treatment to assess therapeutic efficacy and toxicity, respectively. We reasoned that using a cell line that displayed moderate sensitivities to OV-induced and TAC-mediated cytolysis would reveal therapeutic benefit to the combinatorial therapy. In the MDA-MB-231 xenograft tumor models, loading of virus imparted no advantage to the TAC-T cells relative to TAC-T cells alone (**Figure 14A**). All tumors treated with mock-loaded, vector control-T cells continued to grow out following ACT (**Figure 14A**, black). Alternatively, tumors treated with mock-loaded TAC-T cells began to regress between days 4-6 following the first infusion of ACT (ACT I; **Figure 14A**, blue). The smallest tumor from this treatment group continued to regress until day 20 post-ACT I and remained in remission until day 27 post-ACT I (when this study was ended); the other four tumors in this treatment group grew back out starting 14 days post-ACT. Vector control-engineered T cells loaded with MRB-MG1-FLuc could induce regression between 4-10 days post-ACT I (**Figure 14A**, green), with three of five tumors continuing to regress until these mice reached endpoint (14-23 days post-ACT I). Finally, MDA-MB-231 tumors treated with TAC-T cells loaded with MRB-MG1 induced regression between days 6-8 post-ACT I (**Figure 14A**, red). Tumor control was achieved for at least 10 days in this treatment group until reaching endpoint or the end of the study, with only one mouse experiencing tumor outgrowth. Overall, we observed no appreciable difference in tumor growth between mice treated with mock-loaded TAC-T cells and OV-loaded TAC- or vector control-T cells. As such, the tumor killing capabilities of either TAC-T cells or MRB-MG1 was being impaired by the other modality, but it was unclear whether MRB-MG1 negatively impacted upon the

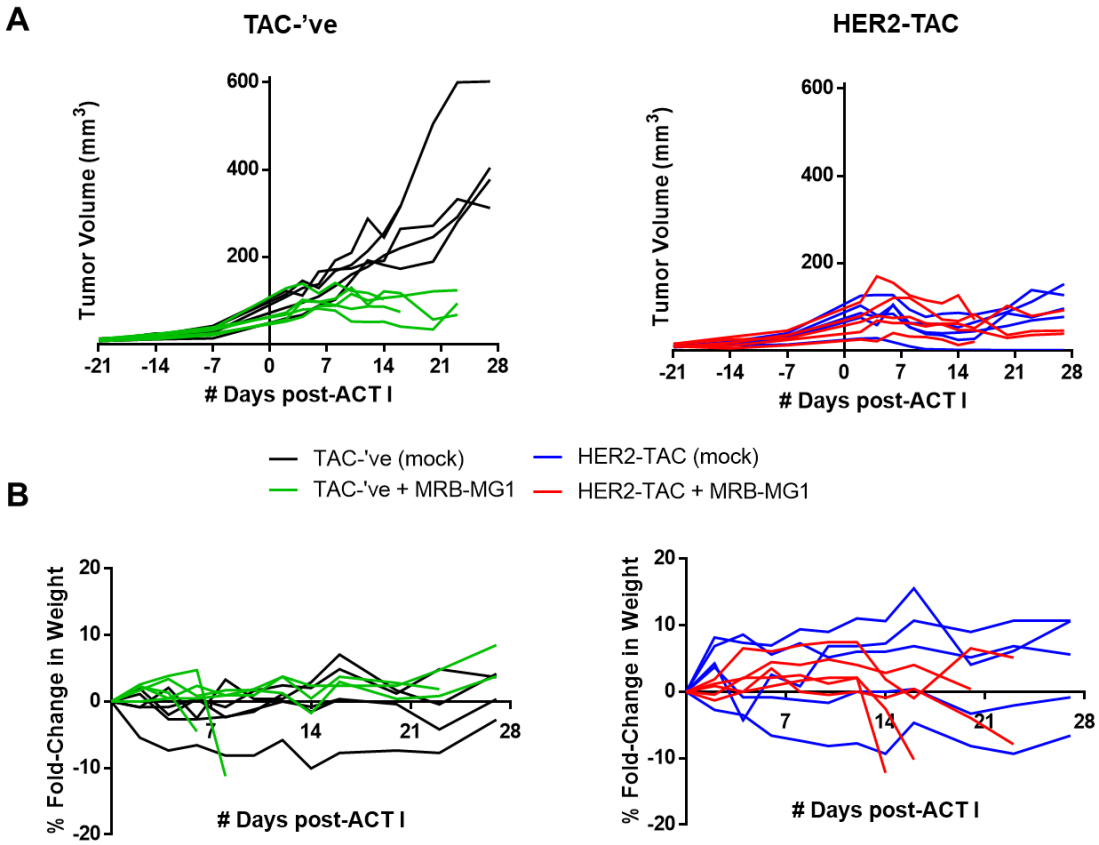

Figure 14: Tumor and weight monitoring following treatment of mice bearing MDA-MB-231 xenograft tumors with OV-loaded, engineered T cells. Mice were inoculated s.c. with $1x10^6$ MDA-MB-231 tumor cells 28 and 30 days following tumor inoculation, mice were treated with engineered T cells, either loaded at an MOI of 3, or mock-loaded with MRB-MG1-FLuc at an MOI of 3. Mice were treated i.v. with two doses of $1x10^7$ OV-loaded HER2-TAC-T cells (red), mock-loaded HER2-TAC-T cells (blue), OV-loaded vector control-T cells (green), or mock-loaded vector control-T cells (black). Following ACT, mice were monitored for tumor volume (**A**) and weight (**B**). Data are representative of 3 independent experiments.

activity of TAC-T cells or if the presence of TAC-T cells impacted upon the activity of MRB-MG1.

We also performed this experiment in an OVCAR-3iv xenograft tumor model, which has greater sensitivity to TAC-T cell mediated cytolysis. We reasoned that this model would reveal any negative effects of the OV on TAC-T cell therapy. Therapy could not be assessed in this model because only one mouse from each group treated with engineered T cells loaded with MRB-MG1 survived past two weeks, apparently due to viral replication in the central nervous system (CNS) (**Figure 12A, 15C**). MRB-MB1 is neurotropic and readily infects the neural tissues of mice lacking a functional immune system. Indeed, in both xenograft tumor models, greater than half of the mice treated with engineered T cells loaded with MRB-MG1 succumbed to lethal toxicities within 16 days of ACT (**Figures 12, 14, 15**).

To limit the dissemination of the virus in the NRG mice, we attempted adoptive transfer of anti-MRB-MG1 neutralizing serum. Neutralizing anti-MRB-MG1 immune sera was generated from wild-type C57Bl/6 mice immunized with MRB-MG1. The presence of anti-MRB-MG1 neutralizing antibodies in this serum was confirmed on VERO cells (**Figure 16**). The neutralizing serum was infused into tumor-bearing mice treated with OV-loaded, engineered T cells to prevent virus dissemination to the CNS. To determine a dose of serum that would prevent CNS replication, mice bearing s.c. MDA-MB-231 xenograft tumors were treated with various doses of immune serum prior to ACT. Two doses of $1x10^7$

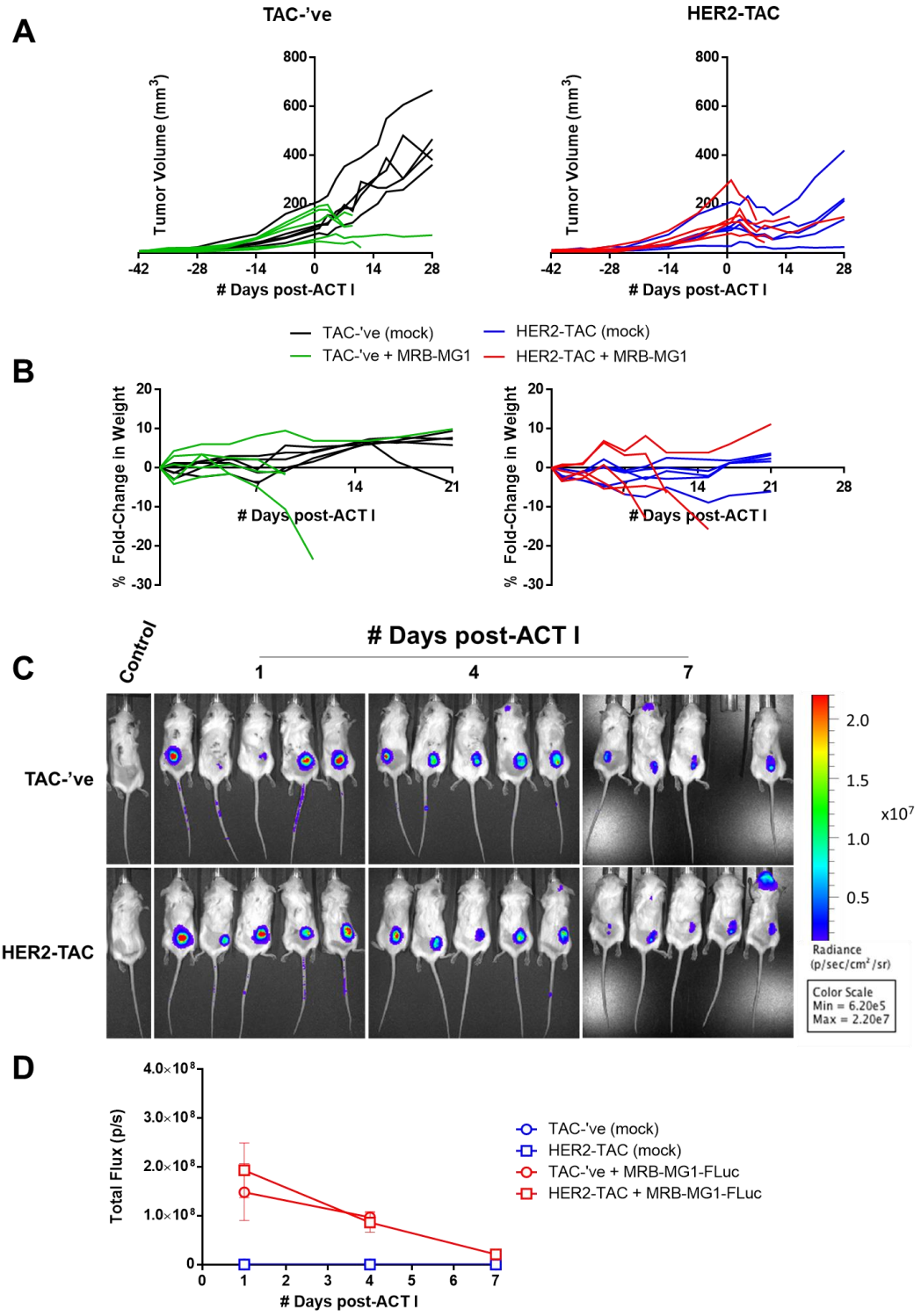
A
TAC-'ve
HER2-TAC
Tumor Volume (mm3)
800
600
400
200
-42
-28
-14
0
14
28
Days post-ACT I
B
TAC-'ve (mock)
TAC-'ve + MRB-MG1
HER2-TAC (mock)
HER2-TAC + MRB-MG1
% Fold-Change in Weight
20
10
0
-10
-20
-30
14
21
28
Days post-ACT I
C
Control
Days post-ACT I
1
4
7
TAC-'ve
HER2-TAC
2.0
1.5
1.0
0.5
x10^7
Radiance (p/sec/cm²/sr)
Color Scale
Min = 6.20e5
Max = 2.20e7
D
Total Flux (p/s)
4.0×10^8
3.0×10^8
2.0×10^8
1.0×10^8
0
0
1
2
3
4
5
6
7
Days post-ACT I
TAC-'ve (mock)
HER2-TAC (mock)
TAC-'ve + MRB-MG1-FLuc
HER2-TAC + MRB-MG1-FLuc

Figure 15: *in vivo* monitoring following treatment of mice bearing OVCAR-3iv xenograft tumors with OV-loaded, engineered T cells. Mice were inoculated s.c. with $1x10^6$ OVCAR-3iv tumor cells. 42 and 44 days following tumor inoculation, mice were treated i.v. with two doses of $1x10^7$ engineered T cells, either mock-loaded, or loaded at an MOI of 3 with MRB-MG1-FLuc. Mice were treated with OV-loaded HER2-TAC-T cells (red), mock-loaded HER2-TAC-T cells (blue), OV-loaded vector control-T cells (green), or mock-loaded vector control-T cells (black) Following ACT, mice were monitored for tumor volume (**A**) and weight (**B**). Mice were monitored for viral replication by visualizing FLuc production via IVIS imaging (**C**). Total flux was calculated using LivingImage software for signal detected in tumors (**D**). Data are presented as mean ± SEM (n = 5). All data represent one individual experiment.

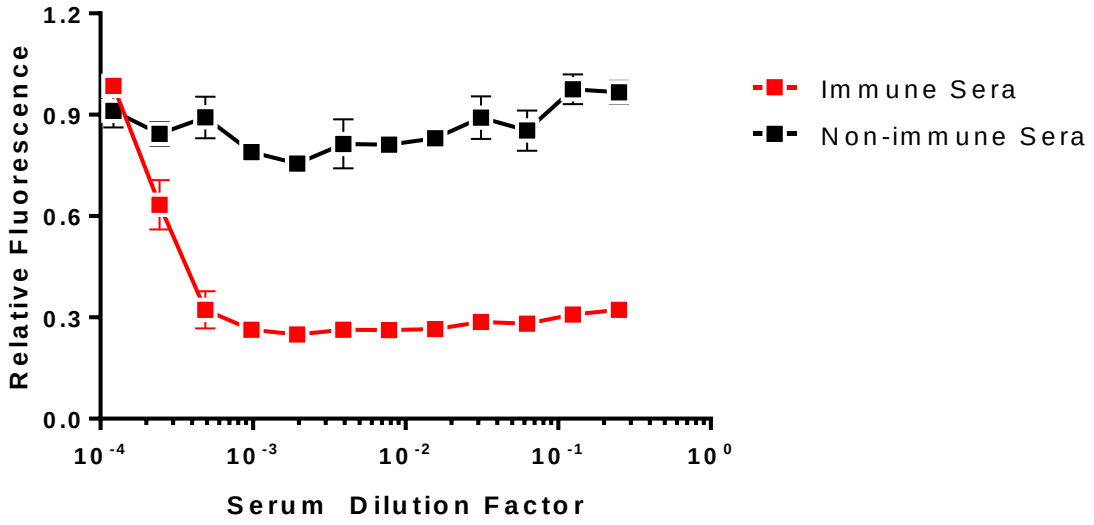

Figure 16: Virus-neutralizing antibody titers. C57BL/6 mice were treated i.v. with $1x10^8$-$1x10^9$ PFU MRB-MG1 (red) or PBS (black) and terminally bled to collect and isolate serum. Serial dilutions of pooled sera were plated in duplicate on VERO cells and treated with $1x10^4$ PFU MRB-MG1 to titrate anti-MRB-MG1 neutralizing antibodies. Plates were incubated overnight and imaged the following day for GFP production on the Typhoon imager. Data were quantified using ImageQuant and are presented as mean, normalized to wells treated with no serum. Data are representative of two individual experiments.

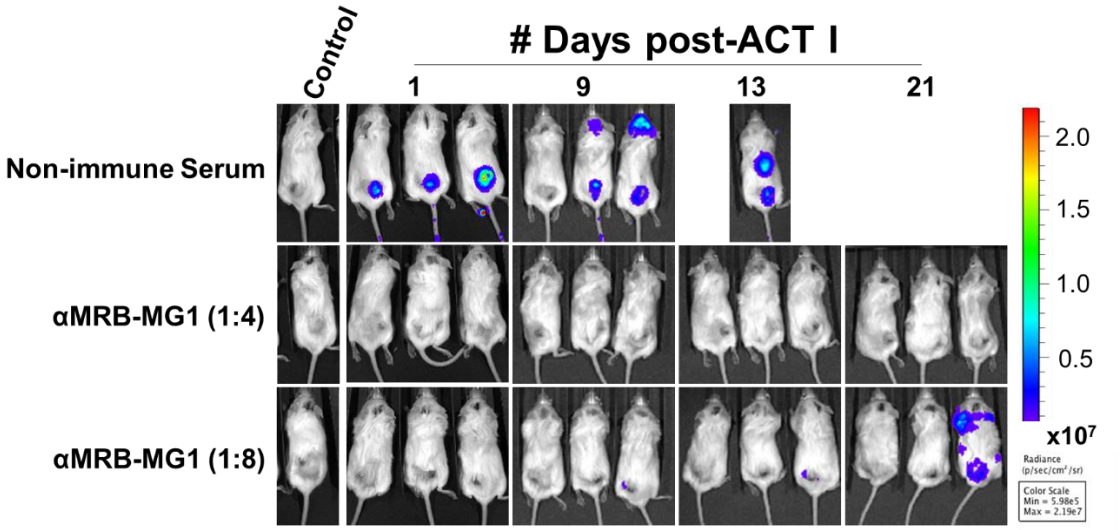

Figure 17: IVIS imaging of MRB-MG1 replication following deposition by vector control-engineered T cells in the presence of anti-MRB-MG1 neutralizing antibodies. Mice were inoculated s.c. with $1x10^6$ MDA-MB-231 tumor cells. Tumor-bearing mice were treated i.v. with two doses of $1x10^7$ engineered T cells, either mock-loaded or loaded at an MOI of 3 with MRB-MG1-FLuc. Anti-MRB-MG1 immune serum generated from wild-type C57BL/6 mice was used to passively immunize tumor-bearing NRG mice one day prior to ACT. Following treatment, mice were imaged over time to detect viral replication by visualizing FLuc production using IVIS imaging. Images represent one individual experiment.

vector control-engineered cells, loaded as described with MRB-MG1-FLuc, were then adoptively transferred into mice 48 hours apart. Mice were monitored following treatment for viral replication by detecting luciferase expression using IVIS imaging (**Figure 17**). The neutralizing serum prevented virus replication in all mice given the serum at a 1:4 dilution and 2/3 mice at a 1:8 dilution (**Figure 17**). Virus replication, measured as luminescence, was only detected in one mouse treated with immune serum at a 1:8 dilution in PBS at 21 days post-ACT. The control mice that received non-immune serum prior to treatment with OV-loaded TAC-T cells displayed virus replication in both the tumor and the CNS. These data indicated that the neutralizing serum can be used to passively protect immunodeficient mice from neural MRB-MG1 infection, but the titers of serum used in this study were too high to allow viral infection of the tumor.

We noticed that viral replication within the brain only occurred following replication within the tumor, indicating that this was a secondary infection following viremia. We reasoned that we could instead prevent secondary infection in the CNS by infusing neutralizing serum after virus replication began in the tumor. Mice bearing s.c. MDA-MB-231 tumors were treated with 2 doses of engineered T cells loaded with MRB-MG1-FLuc as described previously. Following ACT, mice were monitored for viral replication by IVIS imaging. Once a luminescent signal was detected in murine tumors, immune serum was injected i.p. into mice. Mice were monitored for viral replication (**Figure 18**), tumor volume, and weight (**Figure 19**) following treatment. In all mice treated with engineered cells loaded with MRB-MG1-FLuc, viral replication within the tumor was

detected starting one day post-ACT I (**Figure 18A**). Two of the mice in this treatment group reached endpoint within 15 days of ACT, with only one mouse surviving past 25 days (data not shown). Viral infection of the brain was detected in two mice treated with MRB-MG1-loaded, vector control-engineered T cells at 9 days post-ACT I and in one additional mouse before mice succumbed to toxicities (**Figure 19**). These results indicated that the inclusion of neutralizing serum does not prevent virus replication in the CNS.

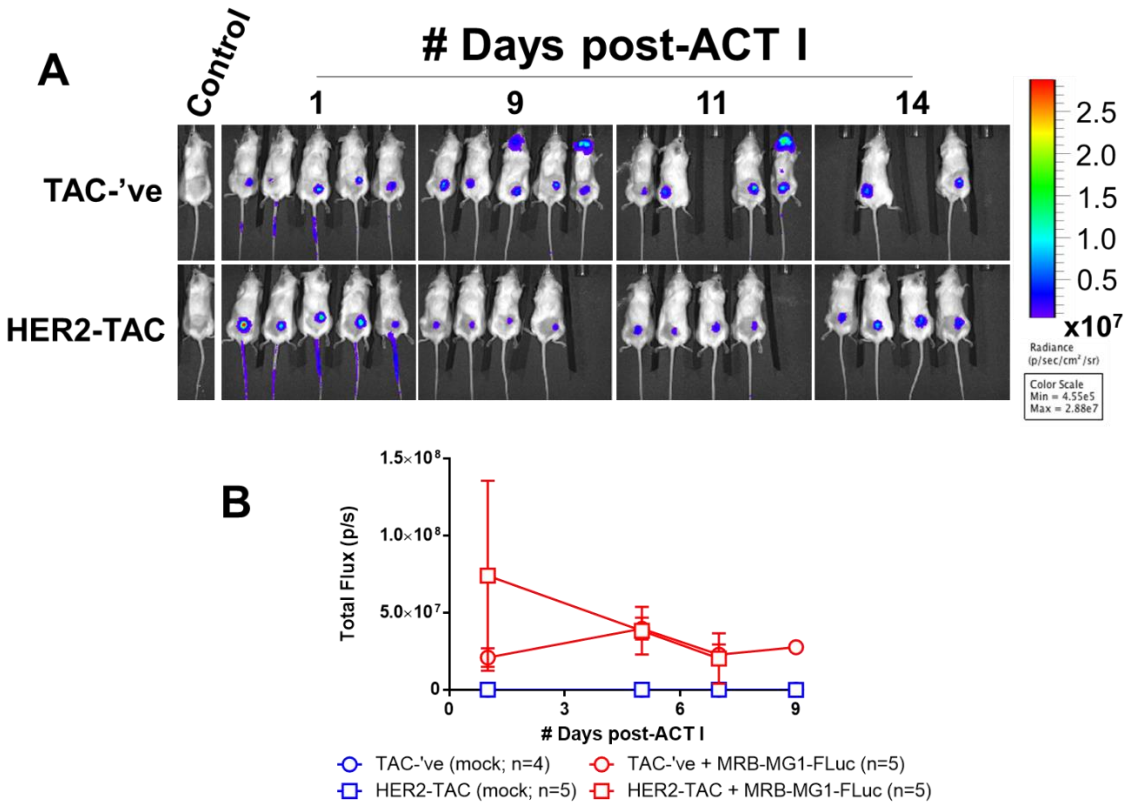

Figure 18: The ability of anti-MRB-MG1 immune serum to prevent viremia following viral deposition by engineered T cells in the tumor. Mice were inoculated s.c. with $1x10^6$ MDA-MB-231 tumor cells. Tumor-bearing mice were treated with HER2-TAC- (squares) or vector control-engineered T cells (circles), either mock-loaded (blue) or loaded at an MOI of 3 with MRB-MG1-FLuc (red). Starting at 28 days post-tumor inoculation, mice were treated i.v. with two doses of $1x10^7$ OV-loaded HER2-TAC-T cells 48 hours apart. Anti-MRB-MG1 Immune serum generated from wild-type C57BL/6 mice was used to treat tumor-bearing NRG mice once viral infection was observed in the tumors of these mice by IVIS imaging. Following treatment, mice were imaged for viral replication by detecting FLuc production by IVIS imaging (A). Total flux was calculated using LivingImage software for signal detected in tumors (B). Data are presented as mean ± SD. All data represent one individual experiment.

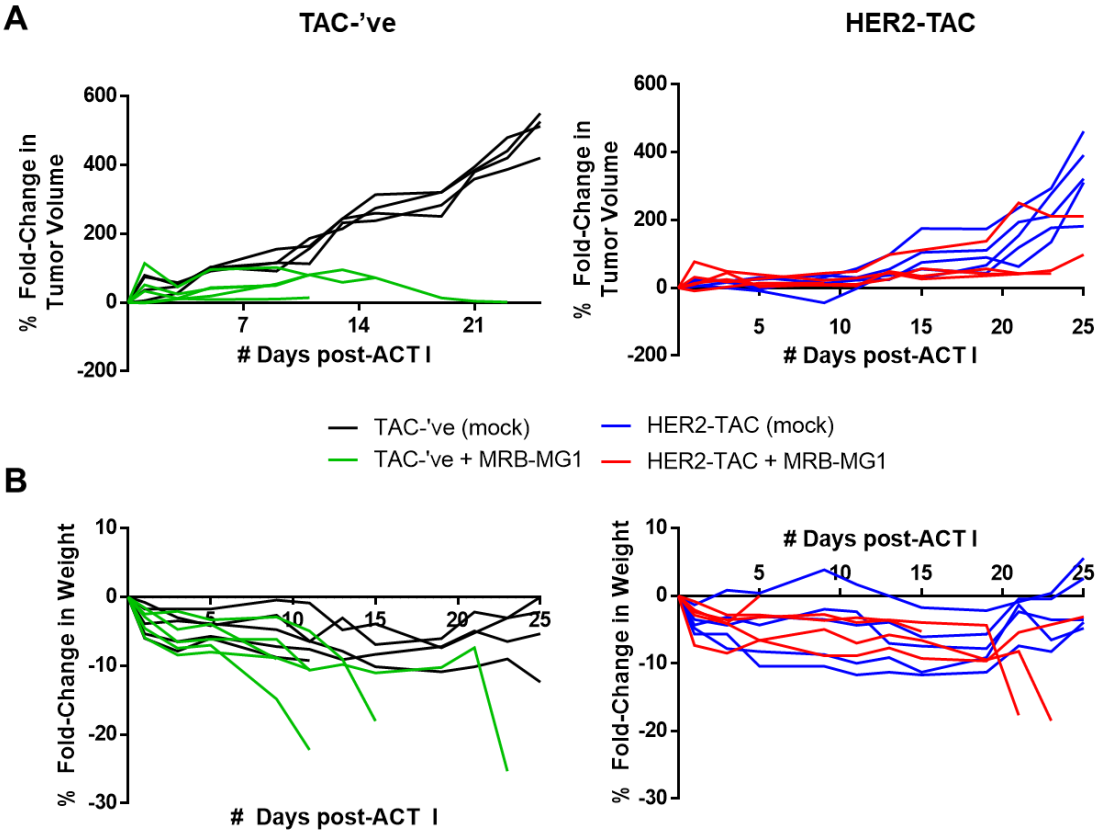

Figure 19: Antitumor efficacy of MRB-MG1-loaded TAC-T cells in the presence of anti-MRB-MG1 neutralizing antibodies. Mice were inoculated s.c. with $1x10^6$ MDA-MB-231 tumor cells. 28 and 30 days following tumor inoculation, mice were treated i.v. with engineered T cells, either mock-loaded, or loaded at an MOI of 3 with MRB-MG1-FLuc. Mice were treated i.v. with two doses of $1x10^7$ OV-loaded HER2-TAC-T cells (red), mock-loaded HER2-TAC-T cells (blue), OV-loaded vector control-T cells (green), or mock-loaded vector control-T cells (black) 48 hours apart. Mice were monitored for viral replication by IVIS imaging Once viral infection was observed in the tumors of these mice, immune serum generated from wild-type C57BL/6 mice was injected i.p. Following treatment, mice were monitored for tumor volume (A) and weight (B). Data are representative of one independent experiment.

5.0 Discussion

The field of immuno-oncology has made tremendous advances in the treatment of cancer, specifically in the use of ACT and OVs as therapeutics. ACT has shown unprecedented promise in treating hematological malignancies[90,91], but solid tumors provide significant challenge to these therapies[149]. Moreover, the use of OVs is another promising modality, with viruses like adenovirus[117] showing efficacy in phase III trials, and herpesvirus (talimogene laherparepvec; T-VEC) being approved for use in the clinic[150]. However, many OV therapies are delivered in high doses for systemic delivery, which poses a risk for unwanted toxicities, or at lower doses via i.t. administration, which is challenging with metastatic disease. As such, there is substantial room to improve upon either of these therapeutic modalities. The next generation of cancer immunotherapies will likely rely on a multi-faceted approach to cancer eradication. OVs possess a natural ability to associate with circulating immune cells, and as such, the concept of using carrier cells for viral delivery was developed.

The use of T cells to deliver OVs has been addressed in previous studies using both transgenic[128,132,151], and CAR-engineered T cells[139]. Engineering T cells with chimeric receptors allows for the re-targeting of bulk T cell populations and avoids MHC-restriction encountered by endogenous T cells. In particular, CAR-engineered T cells were able to carry and deliver VSV to tumor targets, which resulted in enhanced efficacy compared to either therapy used alone. However, the ideal cellular carrier has yet to be identified. Our lab developed a novel chimeric receptor for T cell engineering – the TAC receptor - that

redirects the T cell's native TCR complex upon recognition of target antigen. TAC-engineered T cells were shown to possess increased cytolytic activity with reduced levels of cytokine production and toxicity in various tumor models compared to T cells engineered with a CAR containing an equivalent antigen-binding domain[142]. As such, we reasoned that the properties of TAC-T cells make them ideally suited for use as cellular carriers for OV-delivery.

The concept of viral-loading is attractive from a manufacturing perspective. Loading MRB-MG1 onto TAC-T cells was found to be an innocuous process, as loading of MRB-MG1 had no substantial impact on the phenotype (**Figure 4)** and a modest impact on the functionality (**Figures 4-6, 13**) of these cells *in vitro*. Furthermore, the effective MOI of MRB-MG1 following loading of TAC-T cells was low, suggesting that this multimodal approach can enhance delivery of OV to tumors by reducing the dose of virus required for systemic delivery of naked virions.

A potential concern for the combination of OVs with ACT is the potential for OVs to infect their carrier cell. OVs are unable to infect resting T cells, but can infect these cells following activation[134,152]. Our studies showed that low levels of TAC-engineered T cells, stimulated with cognate antigen, were susceptible to viral infection. However, antigen stimulation did not seem to increase infection and the proportion of infected cells abated over time, suggesting an abortive infection. Indeed, in previous studies, activated T cells loaded with oncolytic measles virus expressed virally-encoded GFP, but did not develop cytopathic effects or release infectious virions[134]. Furthermore, the level of reporter gene

expression observed in TAC-T cells loaded with MRB-MG1-GFP was equivalent to that observed in TAC-T cells exposed to antigen-negative tumor cells or vector control-engineered T cells, demonstrating that cognate interaction does not impair the ability of MRB-MG1 to infect T cells. Taken together, these TAC-T cells are well-suited for OV-delivery – the lack of a productive infection limits the chance of viral vectors eliminating the therapeutic T cells following tumor delivery.

Our *in vitro* data support the use of OV-loaded TAC-T cells to treat a variety of different tumors, which possess varying levels of sensitivity to OV- or TAC-T cell-mediated killing. Tumors that exhibit resistance to either TAC- or OV-mediated cytolysis may be targeted by the other, and tumors possessing some degree of susceptibility to each modality can be killed readily by combining the two therapies. OVCAR-3iv tumor cells were robustly sensitive to TAC-T cell-mediated killing and the addition of OV-loading had no measurable impact on this effect (**Figure 13C)**. TAC-T cells possessed moderate anti-tumor activity against MDA-MB-231 tumor cells, which are marginally sensitive to MRB-MG1 delivered by vector control-T cells (**Figure 13B)**. Furthermore, the ability of these TAC-T cells to kill MDA-MB-231 tumor targets was not impaired following the combination of MRB-MG1-loading with TAC-T cells. A549 tumor cells were minimally sensitive to TAC-T cell-mediated cytolysis, but were successfully eliminated when MRB-MG1-loading was incorporated with these T cells (**Figure 13A**). These data suggest that OV-loaded TAC-T cells may have utility in treating heterogeneous tumors. Although we observed no enhanced therapeutic effect in these tumor cells when MRB-MG1 was

delivered by TAC-T cells *in vitro* compared to that induced by TAC-T cell therapy alone, this combination may still retain utility in the clinic against tumors with differing sensitivities to TAC-mediated cytolysis. Even in experimental instances representing cases where adoptively transferred engineered T cells were functionally ineffective – OV-loaded, vector control-T cells against HER2-expressing tumor targets (**Figure 13**, top panels) or OV-loaded TAC-T cells against targets that do not express HER2 (**Figure 3**) – the presence of MRB-MG1 allowed killing of tumor targets, supporting the fact that OV-loading mitigates the risk infusing patients with T cells that are therapeutically inert following injection, despite showing anti-tumor activity *in vitro.*

OVs associated with cellular carriers must reach the tumor to elicit their anti-tumor activity. Our engineered T cells were unable to deliver OV in the presence of passively-transferred neutralizing antibodies (**Figure 17**). We suspect the high MOI of viral loading is attributable to the lack of OV reaching the tumor following ACT. TAC-T cells in these studies were loaded with OV at an MOI of 3. Previous reports indicated that the efficiency of viral delivery was decreased in immunocompetent models when T cells were loaded at high MOIs (>1) compared to those loaded at low MOIs (<1)[133]. It is likely that at higher MOIs, the threshold at which OV can be concealed from neutralizing antibodies is reached, preventing delivery to the tumor. This requirement for a low MOI at the time of viral loading is ideal, as it reduces the amount of therapeutic virus required for systemic delivery to the tumor.

We failed to distinguish an advantage to using MRB-MG1-loaded TAC-T cells over mock-loaded TAC-T cells *in vivo*. We suspect that limitations in our *in vivo* models are predominantly attributable to the NRG mice used in these studies, which lack a functional immune system and, thus, experience MRB-MG1-mediated neurotoxicity, reaching endpoint before any discernable difference in tumor eradication can be observed. These toxicities are not concerning, as MRB-MG1 has shown to be safe when administered to humans in phase I clinical trials, with some patients presenting with mild, flu-like symptoms[115].

The lack of an observable synergistic or additive anti-tumor response may be attributable to these immunodeficient mice that are unable to elicit endogenous antitumor immunity. Indeed, recent studies have shown that the induction of endogenous antitumor immunity is the primary means by which OVs achieve tumor eradication[107]. Impaired MRB-MG1 replication observed following deposition by TAC-T cells compared to replication following deposition by vector control-T cells likely also contributed to the lack of a difference in therapeutic efficacy; however, this combination may elicit additive or synergistic anti-tumor efficacy in the context of a functional host immune response. This way, MRB-MG1 would not only be able to induce direct tumor cytolysis, but also eradicate tumors by activating endogenous host anti-tumor immunity. In turn, this bystander immunity may provide immunostimulatory molecules, such as IL-15, that can serve to improve the survival of adoptively transferred, engineered T cells[153]. Therefore, seeding a productive infection throughout the entirety of the tumor should be sufficient to promote

the induction of these indirect mechanisms of tumor killing and result in improved therapeutic benefit.

Although we observed impaired MRB-MG1 replication following deposition by TAC-T cells compared to OV replication following deposition by vector control-T cells, viral replication, indicating a productive infection, was still observed following delivery by TAC-T cells for several days post-ACT (**Figures 12A, 15C**). Importantly, loading TAC-T cells with MRB-MG1 did not impair the functionality of the T cells. Taken together, OV-loading of TAC-T cells could provide benefit as a combination therapy.

The combination of these therapies has the potential to provide complementary benefits to each treatment modality. The induction of endogenous immune responses can protect against antigen-loss and prolong the anti-tumor response[108] – this bystander immunity is targeted against additional tumor antigens released upon oncolysis. Viral replication within the tumor additionally promotes vascular shutdown[154]. OVs have been shown to sustain the activated state of adoptively-transferred cells in murine studies of ACT[143]. In return, packaging of OV onto a T cell carrier allows the therapeutic vector to be protected from host-mediated neutralization and delivered directly to the tumor. An additional advantage to OV-loading is that both virus and T cells arrive in the tumor simultaneously, mitigating the chance of OV-induced vascular shutdown that restricts infiltration of these T cells within the tumor. As such, these therapies exhibit complementary characteristics.

There are limitless approaches to combination immunotherapies, and as such, a strategy for determining and evaluating the most relevant and promising combinations is crucial. These treatment modalities can further be combined with preconditioning chemotherapy or irradiation, which have been shown to significantly enhance the engraftment of adoptively transferred cells[155,156]. Not only are these preconditioning regimes beneficial to the adoptively transferred cells, but studies have shown that it can also benefit therapeutic virus by enhancing antitumor efficacy while reducing the generation of vector-neutralizing antibodies[157]. OVs can further be modified to incorporate additional, therapeutic genes that serve to enhance TAC-T cell activity. For example, cytokines such as IL-12 and IL-15, which enhance the functionality and survival of engineered T cells, can be encoded within these OVs and expressed upon tumor infection[158,159]. As such, the combination of OVs with ACT represents a foundation in which to investigate additional, combinatorial strategies.

Overall, these studies offer proof-of-concept that loading TAC-engineered T cells with OV is a feasible approach to combination therapies. These studies assist in generating an understanding of the interplay between TAC-T cells and OVs in combination therapies, laying a foundation on which to test other OVs and therapeutic transgenes to enhance T cell function. Future studies should aim to use this combination therapy as a means to enhance T cell persistence and proliferation, while simultaneously permitting OV replication within the tumor. A greater understanding of how the functionality of these immunotherapies changes in the context of combination strategies with other treatment

modalities will ultimately help to discern specific combination strategies for cancer therapy. Paramount to the success of these innovative strategies will be an increased understanding of the mechanisms contributing to tumor initiation, growth, and the generation of resistance to conventional therapies.

References

[1] Statistics, CCSACOC (2017). Canadian Cancer Statistics 2017. *Canadian Cancer Society*, 1–142.

[2] Morrissey KM, Yuraszeck TM, Li CC, Zhang Y, and Kasichayanula S (2016). Immunotherapy and novel combinations in oncology: current landscape, challenges, and opportunities. *Clin. Transl. Sci.* **9**:89-104.

[3] Hanahan D, and Weinberg RA (2011). Hallmarks of cancer: the next generation. C*ell.* **144**:646-674.

[4] Varghese JS, and Easton DF (2010). Genome-wide association studies in common cancers—what have we learnt? *Curr. Opin. Genet. Dev.* **20**:201-209.

[5] Riboli E, Hunt KJ, Slimani N, Ferrari P, Norat T, Fahey M, Charrondière UR, Hèmon B, Casagrande C, Vignat J, Overvad K, Tjønneland A, Clavel-Chapelon F, Thièbaut A, Wahrendorf J, Boeing H, Trichopolous D, Trichopolous A, Vineis P, Palli D, Bueno-de-Mesquita HB, Peeters PHM, Lund E, Engeset D, González CA, Barricarte A, Berglund G, Hallmans G, Day NE, Key TJ, Kaaks R, and Saracci R (2002). European Prospective Investigation into Cancer and Nutrition (EPIC): study populations and data collection. *Public Health Nutr.* **5**:1113-1124.

[6] Kuper H, Boffetta P, and Adami HO (2002). Tobacco use and cancer causation: association by tumour type. *J. Intern. Med.* **252**:206-224.

[7] Pagano JS, Blaser M, Buendia MA, Damania B, Khalili K, Raab-Traub N, and Roizman B (2004). Infectious agents and cancer: criteria for a causal relation. *Semin. Cancer Biol.* **14**:453-471.

[8] Barcellos-Hoff MH, Lyden D, and Wang TC (2013). The evolution of the cancer niche during multistage carcinogenesis. *Nat. Rev. Cancer*. **13**:511-518.

[9] Weinberg RA (2007). *The Biology of Cancer*. Garland Science.

[10] Hanahan D, and Coussens LM (2012). Accessories to the crime: functions of cells recruited to the tumor microenvironment. *Cancer Cell.* **21**:309-322.

[11] Chambers AF, Groom AC, and MacDonald IC (2002). Metastasis: dissemination and growth of cancer cells in metastatic sites. *Nat. Rev. Cancer.* **2:**563-572.

[12] Tu SM, Lin SH, and Logothetis CJ (2002). Stem-cell origin of metastasis and heterogeneity in solid tumours. *Lancet Oncol*. **3**:508-513.

[13] Mukherjee S (2012). *The Emperor of All Maladies: A Biography of Cancer*. Simon and Schuster.

[14] Imai K, and Takaoka A (2006). Comparing antibody and small-molecule therapies for cancer. *Nat. Rev. Cancer*. 6:714-727.

[15] Tannock IF (1998). Conventional cancer therapy: promise broken or promise delayed? *Lancet*. **351***:*SII9-SII16.

[16] Tsuchiya Y, Sawada S, Yoshioka I, Ohashi Y, Matsuo M, Harimaya Y, Tsukada K, and Saiki I (2003). Increased surgical stress promotes tumor metastasis. *Surgery.* 133:547-555.

[17] Glasner A, Avraham R, Rosenne E, Benish M, Zmora O, Shemer S, Meiboom H, and Ben-Eliyahu S (2010). Improving survival rates in two models of spontaneous postoperative metastasis in mice by combined administration of a β-adrenergic antagonist and a cyclooxygenase-2 inhibitor. *J. Immunol*. **184**:2449-2457.

[18] Fortner JG (1993). Inadvertent spread of cancer at surgery. *J. Surg. Oncol.* **53**:191-196.

[19] Demicheli R, Retsky MW, Hrushesky WJ M, Baum M, and Gukas ID (2008). The effects of surgery on tumor growth: a century of investigations. *Ann. Oncol.* **19**:1821-1828.

[20] Ben-Eliyahu S (2003). The promotion of tumor metastasis by surgery and stress: immunological basis and implications for psychoneuroimmunology. *Brain Behav. Immun.* **17**:27-36.

[21] Corrie PG (2008). Cytotoxic chemotherapy: clinical aspects. *Medicine*. **36**:24-28.

[22] Bow EJ (1998). Infection risk and cancer chemotherapy: the impact of the chemotherapeutic regimen in patients with lymphoma and solid tissue malignancies. *J. Antimicrob. Chemother*. **41**:S1-S5.

[23] Gillette EL, Gillette SM. (1995) Principles of radiation therapy. *Semin. Vet. Med. Surg. (Small Anim.)*. **10**:129–134.

[24] Gebski V, Burmeister B, Smithers BM, Foo K, Zalcberg J, Simes J, and Australasian Gastro-Intestinal Trials Group (2007). Survival benefits from neoadjuvant chemoradiotherapy or chemotherapy in oesophageal carcinoma: a meta-analysis. *Lancet Oncol.* **8**:226-234.

[25] Bhatia S, and Sklar C (2002). Second cancers in survivors of childhood cancer. *Nat. Revs. Cancer*. 2:124-132.

[26] Tucker MA, D'Angio GJ, Boice JD Jr, Strong LC, Li FP, Stovall M, Stone BJ, Green DM, Lombardi F, Newton W, Hoover RN, Fraumeni JF Jr, and For The Late Effects Study Group (1987). Bone sarcomas linked to radiotherapy and chemotherapy in children. *N. Engl. J. Med.* **317**:588–593.

[27] Pedersen-Bjergaardd J, Ersböll J, Hansen VL, Sörensen BL, Christoffersen K, Hou-Jensen K, Nissen NI, Knudsen JB, and Hansen MM (1998) Carcinoma of the urinary bladder after treatment with cyclophosphamide for non-Hodgkin's lymphoma. *N. Engl. J. Med.* **318**:1028–1032.

[28] Bhatia S, Robison LL, Oberlin O, Greenberg M, Bunin G, Fossati-Bellani F, and Meadows AT (1996). Breast cancer and other second neoplasms after childhood Hodgkin's disease. *N. Engl. J. Med.* **334**:745–751.

[29] Invader JE (2011). Cells of origin in cancer. *Nature*. **469**:314-322.

[30] Bozic I, Reiter JG, Allen B, Antal T, Chatterjee K, Shah P, Moon YS, Yaqubie A, Kelly N, Le DT, Lipson EJ, Chapman PB, Diaz LA Jr., Vogelstein B, and Nowak MA (2013). Evolutionary dynamics of cancer in response to targeted combination therapy. *Elife.* **2**:e00747.

[31] Finley M (1974). *History of the Peloponnesian war*. Penguin UK.

[32] Silverstein AM (2009). *History of immunology*. John Wiley & Sons, Ltd.

[33] Dunn GP, Bruce AT, Ikeda H, Old LJ, and Schreiber RD (2002). Cancer immunoediting: from immunosurveillance to tumor escape. *Nature Immunol.* **3**:991-998.

[34] Burnet FM. (1957) Cancer: a biological approach. *Brit Med J.* **1**:841-847.

[35] Boshoff C, and Weiss R (2002). AIDS-related malignancies. *Nat. Revs. Cancer.* **2**:373-382.

[36] Schreiber RD, Old LJ, and Smyth MJ (2011). Cancer immunoediting: integrating immunity's roles in cancer suppression and promotion. *Science.* **331**:1565-1570.

[37] Stewart TJ, and Abrams SI (2008). How tumours escape mass destruction. *Oncogene*. **27**:5894-5903.

[38] Shi F, Shi M, Zeng Z, Qi RZ, Liu ZW, Zhang, JY, Yang YP, Tien P, and Wang FS (2011). PD-1 and PD-L1 upregulation promotes CD8+ T-cell apoptosis and postoperative recurrence in hepatocellular carcinoma patients. *Int. J. Cancer.* **128**:887-896.

[39] Pasche B (2001). Role of transforming growth factor beta in cancer. *J. Cell. Physiol.* **186**:153-168.

[40] Gorelik L, and Flavell RA (2002). Transforming growth factor-beta in T-cell biology. *Nat. Revs. Immunol*. **2**:46-53.

[41] Munn DH, and Mellor AL (2007). Indoleamine 2, 3-dioxygenase and tumor-induced tolerance. *J. Clin. Invest*. **117**:1147-1154.

[42] Gallina G, Dolcetti L, Serafini P, De Santo C, Marigo I, Colombo MP, Basso G, Brombacher F, Borrello I, Zanovello P, Bicciato S, and Bronte V (2006). Tumors induce a subset of inflammatory monocytes with immunosuppressive activity on CD8+ T cells. *J. Clin. Invest.* ***116***:2777-2790.

[43] Nishikawa H, and Sakaguchi S (2010). Regulatory T cells in tumor immunity. *Int. J. Cancer.* **127**:759-767.

[44] Murphy K. (2011) *Janeway's Immunobiology.* Garland Science.

[45] Koch U, and Radtke F (2011). Mechanisms of T cell development and transformation. *Ann. Rev. Cell Dev. Biol.* **27**:539-562.

[46] Arstila TP, Casrouge A, Baron V, Even J, Kanellopoulos J, and Kourilsky P (1999). A direct estimate of the human αβ T cell receptor diversity. *Science.* **286**:958-961.

[47] Hogquist KA, Baldwin TA, and Jameson SC (2005). Central tolerance: learning self-control in the thymus. *Nat. Revs. Immunol.* **5**:772-782.

[48] Klein L, Hinterberger M, Wirnsberger G, and Kyewski B (2009). Antigen presentation in the thymus for positive selection and central tolerance induction. *Nat. Revs. Immunol.* **9:**833-844.

[49] Germain RN (2002). T-cell development and the CD4-CD8 lineage decision. *Nat. Revs. Immunol.* **2**:309-322.

[50] Bonilla FA, and Oettgen HC (2010). Adaptive immunity. *J. Allergy Clin. Immunol.* **125**:S33-S40.

[51] Mellman I, and Steinman RM (2001). Dendritic cells: specialized and regulated antigen processing machines. *Cell.* **106**:255-258.

[52] Lanzavecchia A, and Sallusto F (2001). Regulation of T cell immunity by dendritic cells. *Cell.* **106**:263-266.

[53] Toes RE, Ossendorp F, Offringa R, and Melief CJ (1999). CD4 T cells and their role in antitumor immune responses. *J. Exp. Med.* **189**:753-756.

[54] Shedlock DJ, and Shen H (2003). Requirement for CD4 T cell help in generating functional CD8 T cell memory. *Science.* **300**:337-339.

[55] Wang RF (2001). The role of MHC class II-restricted tumor antigens and CD4+ T cells in antitumor immunity. *Trends Immunol.* **22**:269-276.

[56] Barry M, and Bleackley RC (2002). Cytotoxic T lymphocytes: all roads lead to death. *Nat. Revs. Immunol.* **2**:401-409.

[57] Pardo J, Aguilo JI, Anel A, Martin P, Joeckel L, Borner C, Wallich R, Müllbacher A, Froelich CJ, and Simon, MM (2009). The biology of cytotoxic cell granule exocytosis pathway: granzymes have evolved to induce cell death and inflammation. *Microb. Infect.* **11**:452-459.

[58] Zaidi MR, and Merlino G (2011). The two faces of interferon-γ in cancer. *Clin. Cancer Res.* **17**:6118-6124.

[59] Seliger B, Ruiz-Cabello F, and Garrido F (2008). IFN inducibility of major histocompatibility antigens in tumors. *Adv. Cancer Res.* **101:**249-276.

[60] Balkwill F (2009). Tumour necrosis factor and cancer. *Nat. Revs. Cancer.* **9**:361-371.

[61] Hagen TLT, and Eggermont AMM (2003). Solid tumor therapy: manipulation of the vasculature with TNF. *Technol. Cancer Res. Treat.* **2**:195-203.

[62] Russell JH, and Ley TJ (2002). Lymphocyte-mediated cytotoxicity. *Ann. Rev. Immunol.* **20**:323-370.

[63] Pages F, Galon J, Dieu-Nosjean MC, Tartour E, Sautes-Fridman C, and Fridman WH (2010). Immune infiltration in human tumors: a prognostic factor that should not be ignored. *Oncogene*. **29**:1093-1102.

[64] Rosenberg SA, Restifo NP, Yang JC, Morgan RA, and Dudley ME (2008). Adoptive cell transfer: a clinical path to effective cancer immunotherapy. *Nat. Revs. Cancer.* **8**:299-308.

[65] Chiocca EA, and Rabkin SD (2014). Oncolytic viruses and their application to cancer immunotherapy. *Cancer Immunol. Res.* **2**:295-300.

[66] Bitton RJ (2004). Cancer vaccines: a critical review on clinical impact. *Curr. Opin. Mol. Ther.* **6**:17-26.

[67] Scott AM, Wolchok JD, and Old LJ (2012). Antibody therapy of cancer. *Nat. Revs. Cancer.* **12**:278-287.

[68] Balkwill F, and Mantovani A (2001). Inflammation and cancer: back to Virchow? *Lancet.* **357**:539-545.

[69] Yu Z, and Restifo NP (2002). Cancer vaccines: progress reveals new complexities. *J. Clin. Invest.* **110**:289-294.

[70] Kaiser J (2017). Personalized tumor vaccines keep cancer in check. *Science*. **356**:122.

[71] McGray AR, Hallett R, Bernard D, Swift SL, Zhu Z, Teoderascu F, VanSeggelen H, Hassell JA, Hurwitz AA, Wan Y, and Bramson, JL (2014). Immunotherapy-induced CD8+ T cells instigate immune suppression in the tumor. *Mol. Ther.* **22**:206-218.

[72] Pardoll DM (2012). The blockade of immune checkpoints in cancer immunotherapy. *Nat. Revs. Cancer.* **12**:252-262.

[73] Hodi FS, O'day, SJ, McDermott DF, Weber RW, Sosman JA, Haanen, JB, Gonzalez R, Robert C, Schadendorf D, Hassel JC, Arkerley W, van den Eertwegh AJ, Lutzky J, Lorigan P, Vaubel JM, Linette GP, Hogg D, Ottensmeier CH, Lebbè C, Peschel C, Quirt I, Clark JI, Wolchok JD, Weber JS, Tian J, Yellin MJ, Nichol GM, Hoos A, and Urba WJ (2010). Improved survival with ipilimumab in patients with metastatic melanoma. *N. Engl. J. Med*. **2010**:711-723.

[74] Robert C, Long GV, Brady B, Dutriaux C, Maio M, Mortier L, Hassel JC, Rutkowski P, McNeil C, Kalinka-Warzocha E, Savage KJ, Hernberg MM, Lebbè C, Charles J, Mihalcioiu C, Ciarion-Sileni V, Mauch C, Cognetti F, Arance A, Schmidt H, Schadendorf D, Gogas H, Lundgren-Eriksson L, Horak C, Sharkey B, Waxman IM, Atkinson V, and Ascierto PA (2015). Nivolumab in previously untreated melanoma without BRAF mutation. *N. Engl. J. Med.* **372**:320-330.

[75] Wolchok JD, Kluger H, Callahan MK, Postow MA, Rizvi NA, Lesokhin AM, Segal NH, Ariyan CE, Gordon RA, Reed K, Burke MM, Caldwell A, Kronenberg SA, Agunwamba BU, Zhang X, Lowy I, Inzunza HD, Feely W, Horak CE, Hong Q,

Korman AJ, Wigginton JM, Gupta A, and Sznol M (2013). Nivolumab plus ipilimumab in advanced melanoma. *N. Eng. J. Med.* **369**:122-133.

[76] Slamon DJ, Leyland-Jones B, Shak S, Fuchs H, Paton V, Bajamonde A, Fleming T, Eirmann W, Wolter J, Pegram M, Baselga, J, and Norton L (2001). Use of chemotherapy plus a monoclonal antibody against HER2 for metastatic breast cancer that overexpresses HER2. *N. Eng. J. Med.* **344**:783-792.

[77] Schumacher TN, and Schreiber RD (2015). Neoantigens in cancer immunotherapy. *Science*. **348**:69-74.

[78] Simpson AJ, Caballero OL, Jungbluth A, Yao-Tseng C, and Old LJ (2005). Cancer/testis antigens, gametogenesis and cancer. *Nat. revs. Cancer*. **5**:615-625.

[79] Disis ML, and Cheever MA (1996). Oncogenic proteins as tumor antigens. *Curr. Opin. Immunol.* **8**:637-642.

[80] Rosenberg SA, and Dudley ME (2004). Cancer regression in patients with metastatic melanoma after the transfer of autologous antitumor lymphocytes. *Proc. Natl. Acad. Sci.* **101**:S14639-S14645.

[81] Yee C (2013). Adoptive T-cell therapy for cancer: boutique therapy or treatment modality? *Clin. Cancer Res.* **19**:4550-4552.

[82] Dudley ME, and Rosenberg SA (2003). Adoptive-cell-transfer therapy for the treatment of patients with cancer. *Nat. Revs. Cancer.* **3**:666-675.

[83] Morales JK, Kmieciak M, Graham L, Feldmesser M, Bear HD, and Manjili, MH (2009). Adoptive transfer of HER2/neu-specific T cells expanded with alternating gamma chain cytokines mediate tumor regression when combined with the depletion of myeloid-derived suppressor cells. *Cancer Immunol. Immunother.* **58I**941-953.

[84] Muranski P, and Restifo NP (2009). Adoptive immunotherapy of cancer using CD4+ T cells. *Curr. Opin. Immunol.* **21**:200-208.

[85] Ward PL, Koeppen HK, Hurteau T, Rowley DA, and Schreiber H (1990). Major histocompatibility complex class I and unique antigen expression by murine tumors that escaped from CD8+ T-cell-dependent surveillance. *Cancer Res.* **50**:3851-3858.

[86] Bubeník J (2004). MHC class I down-regulation: tumour escape from immune surveillance? *Int. J. Oncol.* **25**:487-491.

[87] Jensen MC, and Riddell SR (2015). Designing chimeric antigen receptors to effectively and safely target tumors. *Curr. Opin. Immunol.* **33**:9-15.

[88] Sadelain M, Brentjens R, and Rivière I (2013). The basic principles of chimeric antigen receptor design. *Cancer Discov.* **3**:388-398.

[89] Garfall AL, Maus MV, Hwang WT, Lacey SF, Mahnke YD, Melenhorst JJ, Zheng Z, Vogl DT, Cohen AD, Weiss BM, Dengel K, Kerr ND, Bagg A, Levine BL, June CH,

and Stadtmauer EA (2015). Chimeric antigen receptor T cells against CD19 for multiple myeloma. *N. Engl. J. Med*. **373**:1040-1047.

[90] Kochenderfer JN, Dudley ME, Feldman SA, Wilson WH, Spaner DE, Maric I, Stetler-Stevenson M, Phan CQ, Hughes MS, Sherry RM, Yang JC, Kammula US, Carpenter R, Nathan DA, Morgan RA, Laurencot C, and Rosenberg SA (2012). B-cell depletion and remissions of malignancy along with cytokine-associated toxicity in a clinical trial of anti-CD19 chimeric-antigen-receptor–transduced T cells. *Blood*. **119**:2709-2720.

[91] Sadelain M (2015). CAR therapy: the CD19 paradigm. *J. Clin. Invest.* **125**:3392-3400.

[92] Davila ML, Riviere I, Wang X, Bartido S, Park J, Curran K, Chung SS, Stefanski J, Borquez-Ojeda O, Olszewska M, Qu J, Wasielewska T, He Q, Fink M, Shinglot H, Youssif M, Satter M, Wang Y, Hosey J, Quintanilla H, Halton E, Bernal Y, Bouhassira DCG, Arcila ME, Gonen M, Roboz GJ, Maslak P, Douer D, Frattini MG, Giralt S, Sadelain M, and Brentjens R (2014). Efficacy and toxicity management of 19-28z CAR T cell therapy in B cell acute lymphoblastic leukemia. *Sci. Transl. Med*. **6**:224ra25.

[93] Dock G (1904). The influence of complicating diseases upon leukaemia. *Am. J. Med. Sci.* **127**:563-592.

[94] Bluming A, and Ziegler J (1971). Regression of Burkitt's lymphoma in association with measles infection. *Lancet.* **298**:105-106.

[95] Patel MR, and Kratzke RA (2013). Oncolytic virus therapy for cancer: the first wave of translational clinical trials. *Transl. Res.* **161**:355-364.

[96] Kaufman HL, Kohlhapp FJ, and Zloza A (2015) Oncolytic viruses: a new class of immunotherapy drugs. *Nat. Rev. Drug Discov.* **14**:642-662.

[97] Hirasawa K, Nishikawa SG, Norman KL, Alain T, Kossakowska A, and Lee PW (2002). Oncolytic reovirus against ovarian and colon cancer. *Cancer Res.* **62**:1696-1701.

[98] Cassel WA, and Garrett RE (1965). Newcastle disease virus as an antineoplastic agent. *Cancer*. **18**:863-868.

[99] Stojdl DF, Lichty BD, tenOever BR, Paterson JM, Power AT, Knowles S, Marius R, Reynard J, Poliquin L, Atkins H, Brown EG, Durbin RK, Durbin JE, Hiscott J, and Bell JC (2003). VSV strains with defects in their ability to shutdown innate immunity are potent systemic anti-cancer agents. *Cancer Cell.* **4**:263-275.

[100] Andtbacka RH, Kaufman HL, Collichio F, Amatruda T, Senzer N, Chesney J, Delman KA, Spitler LE, Puzanov I, Agarwala SS, Milhem M, Cranmer L, Curti B, Lewis K, Ross M, Guthrie T, Linette GP, Daniels GA, Harrington K, Middleton MR, Miller WH Jr, Zager JS, Ye Y, Yao B, Li A, Doleman S, VanderWalde A, Gansert J, and Coffin RS (2015). Talimogene laherparepvec improves durable response rate in patients with advanced melanoma. J. *Clin. Oncol.* **33**:2780-2788.

[101] Brun J, McManus D, Lefebvre C, Hu K, Falls T, Atkins H, Bell JC, McCart JA, Mahoney D, and Stojdl DF. 2010. Identification of genetically modified maraba virus as an oncolytic rhabdovirus. *Mol. Ther.* **18**:1440-1449.

[102] Bauerschmitz GJ, Lam JT, Kanerva A, Suzuki K, Nettelbeck DM, Dmitriev I, Krasnykh V, Mikheeva GV, Barnes MN, Alvarez RD, Dall P, Alemany R, Curiel DT, and Hemminki A (2002). Treatment of ovarian cancer with a tropism modified oncolytic adenovirus. *Cancer Res.* **62**:266-1270.

[103] Haller O, Kochs G, and Weber F (2006). The interferon response circuit: induction and suppression by pathogenic viruses. *Virology.* **344**:119-130.

[104] Seymour LW, and Fisher KD (2016). Oncolytic viruses: finally delivering. *Br. J. Cancer*. **114**:357-361.

[105] Mahoney DJ, and Stojdl DF (2013). Molecular pathways: multimodal cancer-killing mechanisms employed by oncolytic vesiculoviruses. *Clin. Cancer Res.* **19**:758-763.

[106] Breitbach CJ, Arulanandam R, De Silva N, Thorne SH, Patt R, Daneshmand M, Moon A, Ilkow C, Burke J, Hwang TH, Heo J, Cho M, Chen H, Angarita FA, Addison C, McCart JA,Bell JC, and Kirn DH (2013). Oncolytic vaccinia virus disrupts tumor-associated vasculature in humans. *Cancer Res.* **73**:1265-1275.

[107] Lichty BD, Breitbach CJ, Stojdl DF, and Bell JC (2014). Going viral with cancer immunotherapy. *Nat. Revs. Cancer.* **14**:559-567.

[108] Prestwich RJ, Errington F, Diaz RM, Pandha HS, Harrington KJ, Melcher AA, and Vile RG (2009). The case of oncolytic viruses versus the immune system: waiting on the judgment of Solomon. *Hum. Gene Ther.* **20**:1119–1132.

[109] Benencia F, Courrèges MC, Conejo-Garcia JR, Mohamed-Hadley A, Zhang L, Buckanovich RJ, Carroll R, Fraser N, and Coukos G (2005). HSV oncolytic therapy upregulates interferon-inducible chemokines and recruits immune effector cells in ovarian cancer. *Mol. Ther.* **12**:789–802.

[110] Wongthida P, Diaz RM, Pulido C, Rommelfanger D, Galivo F, Kaluza K, Kottke T, Thompson J, Melcher A, and Vile R (2011). Activating systemic T-cell immunity against self tumor antigens to Support oncolytic virotherapy with vesicular stomatitis virus. *Hum. Gene Ther.* **22**:1343–1353.

[111] Russell SJ, Peng KW, and Bell JC (2012). Oncolytic virotherapy. *Nat. Biotechnol.* **30**:658-670.

[112] Su C, Peng L, Sham J, Wang X, Zhang Q, Chua D, Liu C, Cui Z, Xue H, Wu H, Yang Q, Zhang B, Liu X, Wu M, and Qian Q (2006). Immune gene–viral therapy with triplex efficacy mediated by oncolytic adenovirus carrying an interferon-γ gene yields efficient antitumor activity in immunodeficient and immunocompetent mice. *Mol. Ther.* **13**:918-927.

[113] Zhao H, Janke M, Fournier P, and Schirrmacher V (2008). Recombinant Newcastle disease virus expressing human interleukin-2 serves as a potential candidate for tumor therapy. *Virus Res.* **136**:75-80.

[114] Power AT, Wang J, Falls TJ, Paterson JM, Parato KA, Lichty BD, Stojdl DF, Forsyth PA, Atkins H, and Bell JC (2007). Carrier cell-based delivery of an oncolytic virus circumvents antiviral immunity. *Mol. Ther.* **15**:123-130.

[115] Jonker DJ, Hotte SJ, Abdul Razak AR, Renouf DJ, Lichty B, Bell JC, Powers J, Breitbach CJ, Stojdl DF, Stephenson KB, Bramson JL, Hummel J, Lemay CG, Cutz J, Wells J, Eady R, Sun X, Dongsheng Tu, and Dancey J (2017). Phase I study of oncolytic virus (OV) MG1 maraba/MAGE-A3 (MG1MA3), with and without transgenic MAGE-A3 adenovirus vaccine (AdMA3) in incurable advanced/metastatic MAGE-A3-expressing solid tumours: CCTG IND. 214. e14637-e14637.

[116] Senzer NN, Kaufman HL, Amatruda T, Nemunaitis M, Reid T, Daniels G, Gonzalez R, Glaspy J, Whitman E, Harrington K, Goldsweig H, Marshall T, Love C, Coffin R, and Nemunaitis JJ (2009). Phase II clinical trial of a granulocyte-macrophage colony-stimulating factor–encoding, second-generation oncolytic herpesvirus in patients with unresectable metastatic melanoma. *J. Clin. Oncol.* **27**:5763-5771.

[117] Xia ZJ, Chang JH, Zhang L, Jiang WQ, Guan ZZ, Liu JW, Zhang Y, Hu XH, Wu GH, Wang HQ, Chen ZC, Chen JC, Zhou QH, Lu JW, Fan QX, Huang JJ, Zheng X (2004). Phase III randomized clinical trial of intratumoral injection of E1B gene-deleted adenovirus (H101) combined with cisplatin-based chemotherapy in treating squamous cell cancer of head and neck or esophagus. *Chin. J. Cancer.* **23**:1666-1670.

[118] Fisher K. (2006) Striking out at disseminated metastases: the systemic delivery of oncolytic viruses. *Curr. Opin. Mol. Ther.* **8**:301-313.

[119] Harrington K, and Vile R (2006). Virus smuggling, tax evasion and tumor assassination. *Nat. Med.* **12**:507-509.

[120] Tsai V, Johnson DE, Rahman A, Wen SF, LaFace D, Philophena J, Nery J, Zepeda M, Maneval DC, Demers GW, and Ralston R (2004). Impact of human neutralizing antibodies on antitumor efficacy of an oncolytic adenovirus in a murine model. *Clin. Cancer Res.* **10**:7199-7206.

[121] Ikeda K, Wakimoto H, Ichikawa T, Jhung S, Hochberg FH, Louis DN, and Chiocca EA (2000). Complement depletion facilitates the infection of multiple brain tumors by an intravascular, replication-conditional herpes simplex virus mutant. *J. Virol.* **74**:4765-4775.

[122] Ye X, Jerebtsova M, and Ray PE (2000). Liver bypass significantly increases the transduction efficiency of recombinant adenoviral vectors in the lung, intestine, and kidney. *Hum. Gene Ther.* **11**:621-627.

[123] Bessis N, GarciaCozar FJ, and Boissier MC (2004). Immune responses to gene therapy vectors: influence on vector function and effector mechanisms. *Gene Ther.* **11**:S10-S17.

[124] Willmon C, Harrington K, Kottke T, Prestwich R, Melcher A, and Vile R (2009). Cell carriers for oncolytic viruses: Fed Ex for cancer therapy. *Mol. Ther.* **17**:1667-1676.

[125] Pizzato M, Blair ED, Fling M, Kopf J, Tomassetti A, Weiss RA, and Takeuchi Y (2001). Evidence for nonspecific adsorption of targeted retrovirus vector particles to cells. *Gene Ther.* **8**:1088-1096.

[126] Kirn DH, and Thorne SH (2009). Targeted and armed oncolytic poxviruses: a novel multi-mechanistic therapeutic class for cancer. *Nat. Revs. Cancer.* **9**:64-71.

[127] Thorne SH, Negrin RS, and Contag CH (2006). Synergistic antitumor effects of immune cell-viral biotherapy. *Science.* **311**:1780-1784.

[128] Cole C, Qiao J, Kottke T, Diaz RM, Ahmed A, Sanchez-Perez L, Brunn G, Thompson J, Chester J, and Vile, R. G. (2005). Tumor-targeted, systemic delivery of therapeutic viral vectors using hitchhiking on antigen-specific T cells. *Nat. Med.* **11**:1073-1081.

[129] Roy DG, and Bell JC (2013). Cell carriers for oncolytic viruses: current challenges and future directions. *Oncolytic virotherapy.* **2**:47-56.

[130] Kakarla S, and Gottschalk S (2014). CAR T cells for solid tumors: armed and ready to go? *Cancer J.* **20**:151-155.

[131] Ilett EJ, Prestwich RJ, Kottke T, Errington F, Thompson JM, Harrington KJ, Pandha HS, Coffey M, Selby PJ, Vile RG, and Melcher AA (2009). Dendritic cells and T cells deliver oncolytic reovirus for tumour killing despite pre-existing anti-viral immunity. *Gene Ther.* **16**:689-699.

[132] Qiao J, Wang H, Kottke T, Diaz RM, Willmon C, Hudacek A, Thompson J, Parato K, Bell J, Naik J, Chester J, Selby P, Harrington K, Melcher A, and Vile RG (2008). Loading of oncolytic vesicular stomatitis virus onto antigen-specific T cells enhances the efficacy of adoptive T-cell therapy of tumors. *Gene Ther.* **15**:604-616.

[133] Qiao J, Kottke T, Willmon C, Galivo F, Wongthida P, Diaz RM, Thompson J, Ryno P, Barber GN, Chester J, Selby P, Harrington K, Melcher A, and Vile RG (2008). Purging metastases in lymphoid organs using a combination of antigen-nonspecific adoptive T cell therapy, oncolytic virotherapy and immunotherapy. *Nat. Med.* **14**:37-44.

[134] Ong HT, Hasegawa K, Dietz AB, Russell SJ, and Peng KW (2007). Evaluation of T cells as carriers for systemic measles virotherapy in the presence of antiviral antibodies. *Gene Ther.* **14**:324-333.

[135] Pfirschke C, and Schirrmacher V (2009). Cross-infection of tumor cells by contact with T lymphocytes loaded with Newcastle disease virus. *Int. J. Oncol.* **34**:951-962.

[136] Yotnda P, Savoldo B, Charlet-Berguerand N, Rooney C, and Brenner M (2004). Targeted delivery of adenoviral vectors by cytotoxic T cells. *Blood*. **104**:2272-2280.

[137] Morgan RA, Dudley ME, Wunderlich JR, Hughes MS, Yang JC, Sherry RM, Royal RE, Topalian SL, Kammula US, Restifo NP, Zheng Z, Nahvi A, de Vries CR, Rogers-Freezer LJ, Mavroukakis SA, and Rosenberg SA (2006). Cancer regression in patients after transfer of genetically engineered lymphocytes. *Science*. **314**:126-129.

[138] Kottke T, Diaz RM, Kaluza K, Pulido J, Galivo F, Wongthida P, Thompson J, Willmon C, Barber GN, Chester J, Selby P, Strome S, Harrington K, Melcher A, and Vile RG (2008). Use of biological therapy to enhance both virotherapy and adoptive T-cell therapy for cancer. *Mol. Ther.* **16**:1910-1918.

[139] VanSeggelen H, Tantalic DG, Afsahi A, Hammill JA, and Bramson JL (2015). Chimeric antigen receptor–engineered T cells as oncolytic virus carriers. *Mol. Ther. Oncolytics* **2**:15014.

[140] Palmer DC, Balasubramaniam S, Hanada KI, Wrzesinski C, Yu Z, Farid S, Theoret MR, Hwang LN, Klebanoff CA, Gattinoni L, Goldstein AL, Yang JC, and Restifo NP (2004). Vaccine-stimulated, adoptively transferred CD8+ T cells traffic indiscriminately and ubiquitously while mediating specific tumor destruction. *J. Immunol.* **173**:7209-7216.

[141] Ager A, Watson HA, Wehenkel SC, and Mohammed RN (2016). Homing to solid cancers: a vascular checkpoint in adoptive cell therapy using CAR T-cells. *Biochem. Soc. Trans.* **44**:377-385.

[142] Helsen C, Li B, Denisova G, and Bramson JL (2014). Tri-functional T cell receptor antigen coupler (Tri-TAC): a novel method to direct T cells against tumors. *J. Immunother. Cancer* **2**:17.

[143] Ottolino-Perry K, Diallo JS, Lichty BD, Bell JC, and McCart JA (2010). Intelligent design: combination therapy with oncolytic viruses. *Mol. Ther.* **18**:251-263.

[144] Altomonte J, and Ebert O (2012). Replicating viral vectors for cancer therapy: strategies to synergize with host immune responses. *Microb. Biotechnol.* **5**:251-259.

[145] Zufferey R, Dull T, Mandel RJ, Bukovsky A, Quiroz Dulce, Naldini L, and Trono D (1998). Self-inactivating lentivirus vector for safe and efficient in vivo gene delivery. *J. Virol.* **72**:9873–9880.

[146] Dull T, Zufferey R, Kelly M, Mandel RJ, Nguyen M, Trono D, and Naldini L (1998). A third-generation lentivirus vector with a conditional packaging system. *J. Virol.* **72**:8463-8471.

[147] Allan SE, Alstad AN, Merindol N, Crellin NK, Amendola M, Bacchetta R, Naldini L, Roncarolo MG, Soudeyns H, and Levings MK (2008). Generation of potent and stable human CD4+ T regulatory cells by activation-independent expression of FOXP3. *Mol. Ther.* **16**:194-202.

[148] Amendola M, Venneri MA, Biffi A, Vigna E, and Naldini L (2005). Coordinate dual-gene transgenesis by lentiviral vectors carrying synthetic bidirectional promoters. *Nat. Biotechnol.* **23**:108-116.

[149] Newick K, Moon E, and Albelda SM (2016). Chimeric antigen receptor T-cell therapy for solid tumors. *Mol. Ther. Oncolytics.* **3**:16006.

[150] Pol J, Kroemer G, and Galluzzi L (2016). First oncolytic virus approved for melanoma immunotherapy. *Oncoimmunology*. **5**:e1115641.

[151] Thorne SH, Liang W, Sampath P, Schmidt T, Sikorski R, Beilhack A, and Contag CH (2010). Targeting localized immune suppression within the tumor through repeat cycles of immune cell-oncolytic virus combination therapy. *Mol. Ther.* **18**:1698-1705.

[152] Villa NY, Wasserfall CH, Meacham AM, Wise E, Chan W, Wingard JR, McFadden G, and Cogle CR (2015). Myxoma virus suppresses proliferation of activated T lymphocytes yet permits oncolytic virus transfer to cancer cells. *Blood.* **125**:3778-3788.

[153] NISHIO n, Diaconu I, Liu H, Cerullo V, Caruana I, Bouchier-Hayes L, and Savoldo B (2014). Armed oncolytic viruses enhance immune functions of chimeric antigen receptor-modified T cells in solid tumors. *Cancer Res.* **15**:5195-5205.

[154] Breitbach, CJ, Paterson, JM, Lemay, CG, Falls, TJ, McGuire, A, Parato, KA, Stojdl DF, Daneshmand M, Speth K, Kirn D, McCart JA, Atkins H, and Bell JC (2007). Targeted inflammation during oncolytic virus therapy severely compromises tumor blood flow. *Mol. Ther.* **15**:1686–1693.

[155] Dudley ME (2005). Adoptive cell transfer therapy following non-myeloablative but lymphodepleting chemotherapy for the treatment of patients with refractory metastatic melanoma. *Journal of Clinical Oncology* **23**:2346–2357.

[156] Wrzesinski C, Paulos CM, Kaiser A, Muranski P, Palmer DC, Gattinoni L, Yu Z, Rosenberg SA, and Restifo NP (2010). Increased intensity lymphodepletion enhances tumor treatment efficacy of adoptively transferred tumor-specific T cells. *J. Immunother.* **33**:1–7.

[157] Qiao J, Wang H, Kottke T, White C, Twigger K, Diaz RM, Thompson J, Selby P, de Bono J, Melcher A, Pandha H, Coffey M, Vile R, and Harrington K (2008). Cyclophosphamide Facilitates Antitumor Efficacy against subcutaneous tumors following intravenous delivery of reovirus. *Clin. Cancer Res.* **14**:259–269.

[158] Chmielewski M, and Abken H (2012). CAR T cells transform to trucks: chimeric antigen receptor-redirected T cells engineered to deliver inducible IL-12 modulate the tumour stroma to combat cancer. *Cancer Immunol. Immunother.* **61**:1269–1277.

[159] Stephenson, KB, Barra, NG, Davies, E, Ashkar, AA and Lichty, BD (2012). Expressing human interleukin-15 from oncolytic vesicular stomatitis virus improves

survival in a murine metastatic colon adenocarcinoma model through the enhancement of anti-tumor immunity **19**:238–246.